ChemComm

Accepted Manuscript

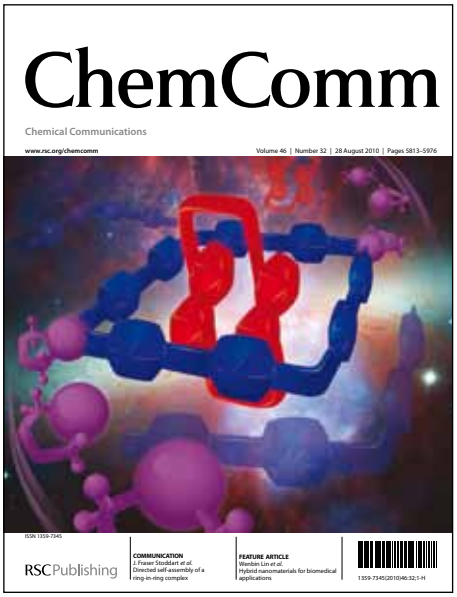

This is an *Accepted Manuscript*, which has been through the RSC Publishing peer review process and has been accepted for publication.

Accepted Manuscripts are published online shortly after acceptance, which is prior to technical editing, formatting and proof reading. This free service from RSC Publishing allows authors to make their results available to the community, in citable form, before publication of the edited article. This *Accepted Manuscript* will be replaced by the edited and formatted *Advance Article* as soon as this is available.

To cite this manuscript please use its permanent Digital Object Identifier (DOI®), which is identical for all formats of publication.

More information about *Accepted Manuscripts* can be found in the **Information for Authors**.

Please note that technical editing may introduce minor changes to the text and/or graphics contained in the manuscript submitted by the author(s) which may alter content, and that the standard **Terms & Conditions** and the **ethical guidelines** that apply to the journal are still applicable. In no event shall the RSC be held responsible for any errors or omissions in these *Accepted Manuscript* manuscripts or any consequences arising from the use of any information contained in them.

Cite this: DOI: 10.1039/c0xx00000x

www.rsc.org/xxxxxx

ARTICLE TYPE

Production of Hydrogen by Electrocatalysis: Making the H-H Bond by Combining Protons and Hydrides

R. Morris Bullock,* Aaron M. Appel, and Monte L. Helm

Received (in XXX, XXX) Xth XXXXXXXXX 20XX, Accepted Xth XXXXXXXXX 20XX
DOI: 10.1039/b000000x

Abstract: Generation of hydrogen by reduction of two protons by two electrons can be catalysed by molecular electrocatalysts. Determination of the thermodynamic driving force for elimination of H_2 from molecular complexes is important for the rational design of molecular electrocatalysts, and allows the design of metal complexes of abundant, inexpensive metals rather than precious metals ("Cheap Metals for Noble Tasks"). The rate of H_2 evolution can be dramatically accelerated by incorporating pendant amines into diphosphine ligands. These pendant amines in the second coordination sphere function as protons relays, accelerating intramolecular and intermolecular proton transfer reactions. The thermodynamics of hydride transfer from metal hydrides and the acidity of protonated pendant amines (pK_a of N-H) contribute to the thermodynamics of elimination of H_2; both of the hydricity and acidity can be systematically varied by changing the substituents on the ligands. A series of Ni(II) electrocatalysts with pendant amines have been developed. In addition to the thermochemical considerations, the catalytic rate is strongly influenced by the ability to deliver protons to the correct location of the pendant amine. Protonation of the amine endo to the metal leads to the N-H being positioned appropriately to favor rapid heterocoupling with the M-H. Designing ligands that include proton relays that are properly positioned and thermodynamically tuned is a key principle for molecular electrocatalysts for H_2 production as well as for other multi-proton, multi-electron reactions important for energy conversions.

Production of hydrogen is of intense interest, particularly since hydrogen is a renewable energy carrier when it is generated from reduction of protons (ideally from water). Solar and wind energy are carbon-neutral, sustainable energy sources, but since they are intermittent, there is a need to convert electricity into chemical energy, such as the H-H bond.[1]

The H-H bond is the simplest chemical bond, so chemists who are not involved in research into H_2 production and utilization may wonder: How hard can it be? Hydrogen has just two electrons and two protons, so it seems simple. Despite this illusion of simplicity, the kinetic barrier for making hydrogen without a catalyst is very high, and therefore many creative approaches to catalysis for hydrogen-evolution have been explored. While the focus of this web theme collection is production of H_2, there is also a need to develop catalysts for the opposite reaction, oxidation of hydrogen. Oxidation of hydrogen occurs in fuel cells, converting the chemical energy of the H-H bond into electrical energy. Oxidation of H_2 also has high barriers in the absence of a catalyst: one-electron oxidation of H_2 is difficult, and the alternative, deprotonation of hydrogen, is also difficult since H_2 is a very weak acid. Thus, it becomes clear that production of hydrogen by reduction of protons, and the reverse reaction, oxidation of H_2, require catalysts to lower the barrier for these reactions.

How should we start thinking about designing a catalyst for electrocatalytic production of H_2? While consideration of the reaction as written in Scheme 1 shows the two protons and

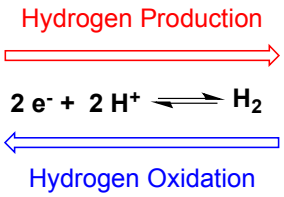

Scheme 1 Two-proton, two-electron production and oxidation of H_2

two electrons, the perspective emphasized here considers the production of H_2 as the heterocoupling of a proton and a hydride (eq. 1). Considering the reaction in this way is advantageous because of the wealth of data available on acidity (proton donor ability) and hydricity (hydride donor ability) of metal hydrides

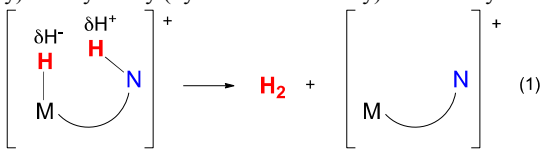

that can provide useful guidance. Both the acidity and hydricity of metal hydrides will be discussed below, providing a framework for understanding the heterocoupling of a proton and hydride to generate H_2.

Hydrogenase enzymes and biologically inspired metal complexes

Nature figured out how to use H_2 as a fuel long before inorganic chemists thought about modeling this reactivity, as hydrogenase enzymes catalyze the production and oxidation of H_2.[2] The two hydrogenase enzymes studied in the greatest detail are the

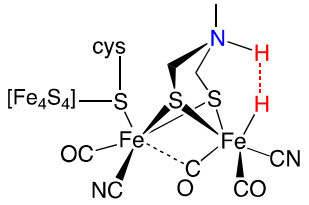

Fig. 2. Proposed structure of the active site of the[FeFe]-hydrogenase, showing formation of the H-H bond.

[FeFe]-hydrogenase and the [NiFe]-hydrogenase; a third type, the [Fe]-hydrogenase has been studied more intensively in recent years.[3] Remarkable progress in protein crystallography[4] led to a much better understanding of the structure of the [FeFe]-hydrogenase enzyme, including the recognition that it is actually an organometallic complex with CO ligands. The structure of the active site is drawn in Fig. 2. This simplified drawing focuses on the Fe_2S_2 core and their ligands, and does not show any of the complexity of the surrounding protein matrix[5] that contributes to their ability to carry out these reactions. A critically important structural feature is the pendant amine that is thought to facilitate proton mobility. Fig. 2 shows the heterolytic cleavage of the H-H bond, poised to deliver a proton to the nitrogen and a hydride ligand to iron. There was considerable amount of debate over the identity of the atom shown as N in Fig 2, but recent studies provided very strong evidence that it is indeed N as shown.[6]

Excellent progress has been made in preparation of synthetic models of the hydrogenase enzymes, where synthetic inorganic complexes are prepared that faithfully model the active site of the enzyme,[2b, 7] providing insight into the function of the enzymes. A wide variety of complexes have been studied that contain the Fe_2S_2 core, often also containing the pendant amines. Pickett and co-workers prepared a structural model of the "H-cluster", including not only the Fe_2S_2 core but also the Fe_4S_4 cluster, and showed that it is an electrocatalyst for proton reduction.[8] Rauchfuss and co-workers synthesized structural models for the [FeFe]-hydrogenase containing pendant amines in the dithiolate bridge,[9] and have compared the reactivity and stability of terminal vs. bridging iron hydrides.[10] The understanding of reactivity provided from their studies led to the synthesis of iron complexes that catalyze the reduction of protons[11] and the oxidation of H_2.[12] Extensive studies by Darensbourg and co-workers on models of the [FeFe]-hydrogenase[13] have led to the development of electrocatalysts for H_2 evolution.[14] Systematic studies of the role of sterically bulky ligands in [FeFe]-hydrogenase model complexes led to new insights about the reactivity in catalysis, particularly for the rotated or "entatic" state of one iron center in the $Fe^{I}Fe^{II}$ form.[15]

Our research focus is on *functional* models of the hydrogenase enzymes, rather than *structural* models. Functional models do not attempt to emulate the structural features of the natural hydrogenase enzymes, but instead are aimed at replicating the catalytic function. A major emphasis in our work is in designing ligands that facilitate the movement of protons,[16] as the formation or oxidation of H_2 requires two protons and two electrons. Protons are much more massive than electrons (by a factor of 1836) so their mobility can be accelerated by the incorporation of bases into the ligand framework. The pendant amines used in our research are designed to function as proton relays that deliver protons to the correct location; they facilitate both intramolecular and intermolecular proton movement. Achieving the optimum advantage from proton relays requires that both the thermodynamics of proton transfer be optimized, as well as the precise positioning of the relay. These considerations will be discussed in detail.

The allure of cheap metals: avoiding precious metal catalysts

Studies of hydrogenase enzymes by biologists and biochemists have led to a greatly increased understanding of their fascinating reactivity. An especially appealing aspect of these enzymes is that they rely on earth-abundant metals like iron and nickel. On the other hand, hydrogenase enzymes are often fragile outside of their native state, which poses limitations on how readily they might ultimately be used in practical devices for production of H_2 or oxidation of H_2. Platinum is an excellent catalyst for oxidation of H_2 in fuel cells, and can also be used for production of H_2. The need to provide energy as a response to increasing worldwide demand,[1a] coupled with efforts to reduce emissions of CO_2 in the atmosphere, requires a decrease in the reliance on fossil fuels. Sustainable energy sources like solar and wind, while attractive and carbon-neutral, will require energy storage on a large scale. Catalysts for efficient conversion between electrical energy and chemical energy are thus needed for a secure energy future, and because of the scale needed, earth-abundant, inexpensive metals are needed. In recent years, increasing efforts have focused on "Cheap Metals for Noble Tasks,"[17] in an effort to design catalysts for H_2 evolution that use inexpensive, abundant metals, such as Ni,[18] Fe,[18d, 19] Co[20] and Mo[21] as alternatives to precious metals like platinum.

Cleavage of the M-H bond of metal hydrides

The fact that a metal *hydride* can be *acidic* might seem paradoxical, but traditional nomenclature refers to complexes with M-H bonds as metal hydrides, regardless of how the M-H bond is formed or cleaved. Metal hydrides were discovered by Hieber in the1930's, but a review of metal hydrides in 1972 pointed out that "hydride complexes of the transition metals remained a laboratory curiosity for a relatively long period of time."[22] Since that time, however, the chemistry of metal hydrides has been extensively developed,[23] first with the exploratory synthetic reactions, then evolving into systematic studies that have led to a more comprehensive understanding of

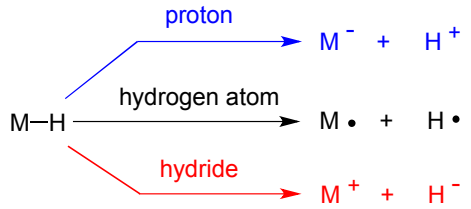

Scheme 2. Cleavage of a metal hydride bond as a proton, hydrogen atom or hydride.

their properties. The M-H bond can be cleaved heterolytically as a proton or a hydride, or homolytically in hydrogen atom transfer reactions.

These three modes of M-H bond cleavage are shown in Scheme 2. The three modes differ in whether the electrons remain on the metal (proton transfer), on the hydride (hydride transfer) or split equally to both (bond homolysis). Hydrogen atom transfer reactions of metal hydrides[24] will not be discussed in detail here, but that type of reactivity continues to be important in several contexts, including applications for organic synthesis.[25]

Free energy vs. enthalpy

Homolytic bond cleavage reactions are frequently reported as enthalpies, often in the gas phase, but for reactions in solution, the solvation energy as well as entropic contributions to a reaction are essential to include for predicting reactivity. For electrochemistry and electrocatalysis, an ion conductive mobile phase is essential, so gas phase reactivity is not as pertinent. Furthermore, electrochemical measurements as well as equilibrium measurements by spectroscopic methods (such as pK_a values by NMR spectroscopy) are free energy measurements, and can be readily converted to standard state values for reaction free energies (reduction potential, bond strengths, etc). From these measurements, there is no need to convert to enthalpy by making assumptions about the entropic term as well as solvation. Bond dissociation enthalpies are useful, and are extensively tabulated for organic compounds in textbooks and other compilations, often based on bond dissociation enthalpies determined from gas phase measurements. For electrocatalysis, the reactions of interest for catalysis are in solution. Despite the prevalence of tabulations of enthalpies, free energies are, in our opinion, more directly pertinent and useful, as they can be directly used to predict whether reactions will actually occur under relevant conditions, because the sign of ΔG makes it immediately clear whether a reaction is favorable in the forward or reverse direction.

Acidity of metal hydrides

Seminal studies by Norton and co-workers in the 1980's provided extremely valuable systematic information on both the kinetic and thermodynamic acidity of metal hydride complexes.[26] These studies were mostly carried out in acetonitrile, which provides a useful comparison to extensive studies of the pK_a values of organic acids in the same solvent.[27] Knowledge of pK_a values are critically needed for the rational design of metal catalysts based on thermodynamic principles, as will be discussed in detail below.

Several trends in the acidity of metal hydrides have been recognized.[26b] The pK_a of 8.3 for the cobalt hydride complex $HCo(CO)_4$ in MeCN indicates that it is a strong acid, being comparable to the acidity of HCl (pK_a about 8.9 in MeCN). Acidity tends to decrease in moving from first or second row metals to third row congeners: the pK_a of 13.9 for $HMo(CO)_3Cp$ shows that it is more acidic than $HW(CO)_3Cp$ (pK_a = 16.1); the difference is even larger when comparing first-row $HMn(CO)_5$ (pK_a = 14.2[26e]) to the third-row complex $HRe(CO)_5$ (pK_a = 21.1). Changes in ligands can result in even larger changes in acidity. Replacement of an electron-withdrawing CO ligand by a electron-donating phosphine lowers the acidity of the metal hydride. The pK_a of 15.4 for $HCo(CO)_3(PPh_3)$ is about 7 pK_a units less acidic compared to $HCo(CO)_4$, while the stronger donor PMe_3 has an even larger effect, with the pK_a of 26.6 being reported for $HW(CO)_2(PMe_3)Cp$. The related tungsten hydride with a strongly donating N-heterocyclic carbene ligand, $CpW(CO)_2(IMes)H$ (IMes = 1,3-bis(2,4,6-trimethylphenyl)-imidazol-2-ylidene) is even less acidic, with a pK_a of 31.9.[28] In addition to the studies on thermodynamic acidity, Norton's studies also showed that the intrinsic barrier to proton transfers to and from metals (forming or breaking the M-H bond) is substantially larger than the barrier to proton transfers to amine bases.[26c] Proton transfer self-exchanges for amine bases like aniline (e.g., degenerate proton transfer from anilinium to aniline) typically occur at diffusion-controlled rates ($k > 10^9$ M^{-1} s^{-1}), while proton transfer self-exchange from $HW(CO)_3Cp$ to its conjugate base, $[W(CO)_3Cp]^-$, occurs with a second-order rate constant of 650 M^{-1} s^{-1} at 25 °C in MeCN.[26c]

Oxidation of a neutral diamagnetic metal hydride can lead to the resulting cationic paramagnetic metal hydride having a greatly enhanced acidity. Tilset and co-workers found that one-electron oxidation of $HM(CO)_3Cp$ (M = Cr, Mo, W) increased the acidity of the M-H bond by about 20.6 (± 1.5) pK_a units in MeCN.[29] For example, oxidation of $HMo(CO)_3Cp$ (pK_a = 13.9) gives the 17-electron radical cation $[HMo(CO)_3Cp]^{+\bullet}$ (pK_a = -6.0). Studies on related Cr hydrides showed a similar trend: one-electron oxidation weakens the M-H bond toward both homolytic cleavage (H• transfer) and heterolytic cleavage (H^+ transfer).[30] A decrease of 21 pK_a units upon oxidation of the metal hydride amounts to an activation of 29 kcal/mol towards proton transfer, while the homolytic (hydrogen atom transfer) mode of cleavage is activated by a much smaller amount (estimated as 8-11 kcal/mol).[30]

DuBois and co-workers have studied the pK_a values of metal hydrides containing two diphosphine ligands. A series of cobalt hydrides containing two dppe ligands [dppe = 1,2-bis(diphenylphosphino)ethane] exhibited a remarkable range of about 27 pK_a units as the oxidation state and charge were changed.[31] The neutral hydride $HCo(dppe)_2$ has a low acidity (pK_a = 38.1), while its conjugate acid, the cationic dihydride $[(H)_2Co(dppe)_2]^+$, is much more acidic (pK_a = 22.8). Oxidation of $HCo(dppe)_2$ gives the much more acidic cationic, paramagnetic hydride $[HCo(dppe)_2]^+$ (pK_a = 23.6). The dicationic hydride, $[HCo(dppe)_2(NCCH_3)]^{2+}$, is the most acidic of this series (pK_a = 11.3).

The pK_a of the Ni hydride complex $[HNi(dppe)_2]^+$ is 14.2 in MeCN,[32] and the pK_a of $[HNi(dmpe)_2]^+$ [dmpe = 1,2-bis(dimethylphosphino)ethane] is much higher (pK_a = 24.3). Thus changing from Ph substituents on phosphorus to the

stronger electron-donating methyl groups in dmpe decreased the acidity of the metal hydride complex by ten orders of magnitude. The high intrinsic barriers for proton transfers from metal hydrides means that such reactions can be slow. In addition, sterically demanding ligands can result in slow deprotonation of metal hydrides because the incoming base encounters large ligands as it approaches the M-H bond. Darensbourg and co-workers[33] found that deprotonation of the cationic metal hydride $[HMo(CO)_2(dppe)_2]^+$ by pyridine is slow, but addition of Cl^- accelerates the reaction by at least a factor of 100. A larger acceleration is observed with F^-, and a smaller acceleration is observed with Br^- or I^-. The halide anion is believed to function as a kinetically active base that deprotonates the metal hydride quickly, then delivers the proton to the amine base. These intermolecular proton transfer reactions provided important early examples where a proton can be relayed using an external base to accelerate proton mobility from a metal hydride complex with sterically demanding diphosphine ligands.

Ott, Lomoth and co-workers studied the protonation of Fe_2 complexes that have pendant amines in an azaditholate bridging ligand.[7x] These complexes are models for the reactivity of the [FeFe]-hydrogenase enzymes. The kinetic site of protonation was at the pendant amine ligand, producing an N-H bond, but the thermodynamically favored site for the proton is a hydride bridging the two irons. The tautomerization was found to be catalyzed by chloride functioning as a kinetic base with little steric hindrance. The kinetics of the protonation of the iron complex was studied by time-resolved IR spectroscopy.

Hydride transfer reactions of metal hydrides: thermodynamic and kinetic hydricity

Understanding of the factors that influence the ability of a metal hydride complex to deliver a hydride (H^-) to a substrate is fundamentally important to the rational design of catalysts that involve hydride transfers. DuBois and co-workers systematically studied the thermodynamic hydricity (hydride donating ability) of a wide range of metal hydrides that have two diphosphine ligands. Thermodynamic hydricity can be measured by several methods;[34] one method commonly used involves a thermodynamic cycle as shown in Scheme 3. The first step is written as the reaction of a metal hydride with an acid to produce

$L_nMH^+ + BH^+ \rightarrow L_nM^{2+} + H_2 + B$	$-1.364 \log K$	eq. 2‡
$B + H^+ \rightarrow BH^+$	$-1.364\ pK_a(BH^+)$	eq. 3
$H_2 \rightarrow H^+ + H^-$	76 kcal/mol	eq. 4
$L_nMH^+ \rightarrow L_nM^{2+} + H^-$	$\Delta G°_{H^-}$	eq. 5

Scheme 3. Thermodynamic Cycle for Determination of Hydricity of Metal Hydrides Using Heterolytic Cleavage of Hydrogen

H_2. Experimentally, the equilibrium is typically measured by carrying out the reaction in the opposite direction (right to left in eq. 2), by adding H_2 gas to a solution containing a metal complex and a base, leading to heterolytic cleavage of H_2 into a proton and a hydride. Regardless of the direction for experiments, showing that the reaction is reversible is essential to demonstrate that equilibrium is reached (which means running the reaction in both directions, or shifting it the opposite direction as part of an experiment). Achieving an equilibrium that can be measured requires a base of appropriate strength. Eq. 3 shows the pK_a of the BH^+, measured in the same solvent (MeCN in all of the examples described here). The free energy of the heterolytic cleavage of H_2 is (the hydricity of H_2) is 76 kcal/mol in MeCN.[34] This value is considerably lower than the free energy of homolytic cleavage of H_2 into two hydrogen atoms in MeCN (103.6 kcal/mol)[35] due to the solvation of the proton and hydride by MeCN, a relatively polar solvent. Representative examples of the thermodynamic hydricity values that have been determined are listed in Table 1.

Table 1. $\Delta G°_{H^-}$ for Hydride Transfer Reactions (eq. 5) in CH_3CN

Metal Hydride	$\Delta G°_{H^-}$ (kcal/mol)[b]	Reference
$HRh(dmpe)_2$	26	[36]
$HW(CO)_4(PPh_3)^-$	36	[37]
$HCo(dmpe)_2$	37	[38]
$[HPt(dmpe)_2]^+$	42	[34]
$HW(CO)_5^-$	40	[37]
$HCo(dppe)_2$	49	[31]
$[HNi(dmpe)_2]^+$	51	[34]
$[HPt(dppe)_2]^+$	53	[32]
$HMo(CO)_2(PMe_3)Cp$	55	[39]
$[HNi(dppe)_2]^+$	63	[32]
$[HPt(EtXantphos)_2]^+$	76	[40]
H_2	76	[34]
$HCPh_3$	96	[41]

[a]dmpe = 1,2-bis(dimethylphosphino)ethane; dppe = 1,2-bis(diphenylphosphino)ethane; EtXantphos = 9,9-dimethyl-4,5-bis(diethylphosphino)xanthene; [b]estimated uncertainties on $\Delta G°_{H^-}$ values are typically ±2 kcal/mol

Remarkably, the range of hydricities for metal hydrides spans 50 kcal/mol, providing substantial flexibility in the design of catalysts that may need either strong or weak hydride donor ability. Note that lower values of $\Delta G°_{H^-}$ correspond to improved hydride donors, similar to lower pK_a values corresponding to better acids. The three principle factors that determine hydricity for $HM(diphosphine)_2^+$ complexes are the substituents on the diphosphine ligand, the metal, and the bite angle of the diphosphine ligand. The hydricity of $[HNi(dmpe)_2]^+$, which has the strongly electron-donating ligand dmpe, exceeds that of $[HNi(dppe)_2]^+$ by 12 kcal/mol. Table 1 shows a difference of 11 kcal for the Pt analogs, and similarly large influences are found for hydrides of Rh,[36, 42] Pd[43] and Co.[31, 38] Large changes in hydricity are also apparent when the metal is changed: the third row metal hydride $[HPt(dmpe)_2]^+$ is a stronger hydride donor by 9 kcal/mol compared to the first row congener $[HNi(dmpe)_2]^+$; the higher hydricity of the second row complex $HRh(dmpe)_2$ compared to its first row analog $HCo(dmpe)_2$ is also shown in Table 1. The rhodium hydride $HRh(dmpe)_2$ is an exceptionally strong hydride donor, being comparable to that of $HBEt_3^-$ (SuperHydride®).[36, 42b] A remarkably large influence of bite angle of the diphosphine on the hydricity was found for a series of Pd hydrides, $[HPd(diphosphine)_2]^+$.[43] The hydricity of this

series of Pd hydrides varied by 27 kcal/mol as the bite angle changed from 78° to 111°. $[Pd(diphosphine)_2]^{2+}$ complexes with small bite angles are square planar. Complexes with larger bite angles are distorted towards a tetrahedral geometry, which stabilizes the LUMO, giving complexes that are more readily reduced, and which bind a hydride more strongly. As a result, $[HPd(diphosphine)_2]^+$ complexes with large bite angles are weaker hydride donors. Theoretical methods have been developed that generally provide good agreement with the large body of experimentally determined values.[44]

Prior to the studies of thermodynamic hydricity of metal hydrides, there were efforts by several groups to study hydride transfer reactions of metal hydrides and to identify trends in reactivity that might reveal the factors that influenced hydricity. Early studies by Labinger and co-workers showed that hydride transfer ability of metal hydrides has some correlation with the position of the metal in the periodic table, decreasing in moving from left to right.[45] The reaction of the group 4 zirconium hydride $[Cp_2ZrH_2]_n$ with acetone occurs rapidly at room temperature, providing $[Cp_2Zr(OCHMe_2)_2]$; subsequent hydrolysis releases isopropyl alcohol. In contrast, the group 5 hydride Cp_2NbH_3 reacted slowly with acetone. The group 6 hydride Cp_2MoH_2 did not react with acetone, even at 78 °C, but it did react with the more electrophilic ketone $(CF_3)(CH_3)C{=}O$. The group 7 hydride Cp_2ReH did not react with either acetone or $(CF_3)(CH_3)C{=}O$. This study provides evidence that hydride transfer ability generally increases in metals towards the left of the periodic table, but possible binding of the ketone to the metal prior to hydride transfer may signal that a combination of factors is involved.

Extensive studies of the synthesis and reactivity of anionic metal carbonyl hydrides were carried out by Darensbourg and co-workers,[46] leading to metal complexes that convert alkyl halides to alkanes,[47] acyl chlorides to aldehydes[48] and ketones to alcohols.[49] The kinetics of conversion of butyl bromide to butane (eq. 6) were studied in THF at 26 °C. The rate constant

$$[M{-}H]^- + Bu{-}Br \longrightarrow [M{-}Br]^- + Bu{-}H \quad (6)$$

for hydride transfer from $[HW(CO)_5]^-$ was $k = 3.3 \times 10^{-3}$ M^{-1} s^{-1}; the rate constant was about 15 times larger ($k \approx 5.0 \times 10^{-2}$ M^{-1} s^{-1}) for $[HW(CO)_4(P(OMe)_3]^-$, which has an electron-donating phosphite ligand on the metal that increases its hydricity.[50]

Hydride transfer reactions of transition metal hydrides are important in the ionic hydrogenation of C=O bonds,[51] which proceed by protonation of a ketone followed by hydride transfer from a metal hydride to generate an alcohol.[52] The kinetics of hydride transfer from metal hydrides to $Ph_3C^+BF_4^-$ was studied by stopped-flow techniques (eq. 7).[53] The metal hydrides studied included metal carbonyl hydrides such as $HW(CO)_3Cp$, $HMo(CO)_3Cp$, and derivatives of these hydrides with more electron-donating phosphine ligands. The hydride transfer from the metal to carbon produces a 16-electron cation, M^+, which is captured by the BF_4^- anion to form a weakly bound ligand.

$$M{-}H + Ph_3C^+\,BF_4^- \xrightarrow{k_{H-}} M{-}F{-}BF_3 + Ph_3C{-}H \quad (7)$$

The rate constants measured spanned a range of $> 10^6$. Third row metal hydrides are faster hydride donors than first row congeners. For example, for hydride transfer to Ph_3C^+, $k = 2 \times 10^3$ M^{-1} s^{-1} for $HRe(CO)_5$, while that for $HMn(CO)_5$ is $k = 50$ M^{-1} s^{-1}. The effect of changing the ligand is much greater than that of changing the metal. An example is that the kinetic hydricity of *trans*-$HMo(CO)_2(PMe_3)Cp$ exceeds that of $HMo(CO)_3Cp$ by a factor of about 10^4.[53a]

Pendant amines as proton relays in nickel(II) complexes

Research in the Center for Molecular Electrocatalysis at Pacific Northwest National Laboratory has focused the key role that proton movement has on reactivity in metal catalysts for production of H_2 and for oxidation of H_2. The emphasis on $Ni(diphosphine)_2^{2+}$ complexes was based on an evaluation of the hydricity of many metal hydride complexes conducted by DuBois and co-workers, in work that began several years before these complexes were shown to have catalytic activity. The careful evaluation of the factors that influence thermodynamic hydricity of metal hydride complexes is applicable to many reactions of metal hydrides, not just the reactivity discussed here that is focused on the production or oxidation of H_2. Before discussing the catalytic activity of these complexes in reduction of protons, stoichiometric reactions of these Ni complexes and thermochemical measurements will be discussed, as they provide insight needed for understanding of the proposed mechanism of the catalytic reactions.

DuBois and co-workers found that the Ni complex $[Ni(PNP)_2]_{2+}$ (PNP = $Et_2PCH_2NMeCH_2PEt_2$) is a functional model for hydrogenase enzymes, as this complex catalyzes the oxidation of H_2. The catalysis occurs at -0.64 V (vs. $Cp_2Fe^{+/0}$), which is about 600 mV more negative than the Ni(II/I) potential of $[HNi(depp)_2]^+$ (depp = 1,2-bis(diethylphosphino)propane), a

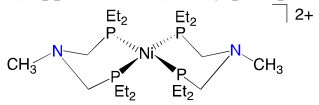

$[Ni(PNP)_2]^{2+}$

Fig. 3 A Ni(II) complex with a "PNP" ligand that has pendant amines.

related complex that has no pendant amines. The very large change in potential resulting from incorporation of the pendant amines indicates coupling of the electron and proton transfer steps. The PNP ligand undergoes chair/boat isomerizations similar to those that occur in cyclohexane rings; consequently the pendant amine is only positioned correctly for interaction with the metal when it is in the boat configuration. Most of the studies reviewed here use "P_2N_2" ligands; the advantage of these ligands is that one of the rings is forced to be in a boat configuration, properly positioning it for interaction with the metal center.[16b]

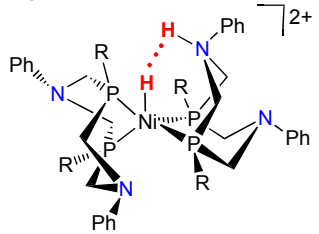

Fig. 4 Key Ni(II) intermediate for production of H_2 using with $[Ni(P^R{}_2N^{R'}{}_2)_2]^{2+}$ electrocatalysts.

Details of the mechanism of H-H bond formation will be discussed later, but the key intermediate is shown in Fig. 4, a complex produced by adding two electrons and two protons to $[Ni(P^R_2N^{R'}_2)_2]^{2+}$, specifically with the geometry shown, with endo protonation of the N-H bond. Critical features that may be tuned are the acidity of the N-H bond and the hydricity of the Ni-H bond. The ensuing discussion will emphasize the heterocoupling of protons (from the N-H) and hydride (from the Ni-H) to form H_2.

Proton reduction using expensive acids?

Research on electrocatalysts for proton reduction to generate H_2 is often carried out using organic acids as the proton source. Use of organic acids has the advantage of being able to select among a variety of acids of different pK_a values and different sterics, providing useful mechanistic information. But sometimes the question is raised of how practical it is to study reduction of protons from organic acids, since they would clearly be prohibitively expensive as stoichiometric reagents for H_2 production. It is important to recognize that electrochemical studies often study "half-reactions." In other words, when studying proton reduction, there must be a corresponding oxidation occurring in the same electrochemical experiment (occurring at the counter electrode in a cyclic voltammogram experiment). In a practical electrolysis cell for the production of H_2, acid is produced from water oxidation and consumed by proton reduction, thereby eliminating the stoichiometric consumption of organic acids used in fundamental studies. For example, in an electrolysis cell, oxidation of water generates protons in one half-reaction (at the anode), and these protons are reduced on the other side of the cell to form H_2 at the cathode (Scheme 4). This balanced production and consumption of H^+ results in zero net change in H^+ for the overall electrolysis cell, and therefore, the stoichiometric depletion of an organic acid is not necessary in the overall process.

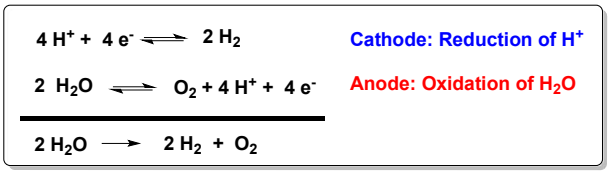

Scheme 4. Reduction of protons to generate H_2 and oxidation of water as the two half-reactions of water splitting.

Many of our studies of the proton reduction half-reaction use $[DMF(H)]^+$, a crystalline acid that is easily prepared by protonation of dimethylformamide with triflic acid (CF_3SO_3H = HOTf).[54] This acid was initially selected for H_2 evolution studies using $[Ni(P^{Ph}_2N^{Ph}_2)_2]^{2+}$ because it is estimated[55] to have the correct pK_a to match that of the protonated pendant amine when the complex is reduced to Ni^I. However, while this acid is well-suited for some of the complexes studied in our lab, different acids and solvents will be optimal for different catalysts. For electrocatalysts that operate in water,[14d, 20b, 20g, 20h, 21b, 21c] the solution acidity is readily changed by adjusting the pH using traditional aqueous pH buffers to prevent large pH excursions (and thereby changes in overpotentials and possibly rates). The principle is the same for reduction of protons in organic solvents, for which acids with varying pK_a values can be used. Ultimately, in a device using these reactions, the aqueous buffers or organic acids would not be stoichiometrically consumed and may not be needed at all.

Addition of H_2 to $[Ni(P^R_2N^{R'}_2)_2]^{2+}$ complexes

Much of the mechanistic insight on Ni catalysts for evolution of H_2 has come from spectroscopic studies of the reverse reaction, oxidation of H_2, in which H_2 is added to Ni(II) complexes. Addition of H_2 to an organometallic or inorganic metal complex can result in the formation of a dihydrogen complex, M(η^2-H_2), where the H_2 ligand is bound to the metal.[56] In other examples, the thermodynamically favored product is a metal dihydride, with two M-H bonds, which may evolve from an initially generated dihydrogen complex that may or may not be observed. In contrast to these typical reactivity patterns, addition of H_2 to $[Ni(P^R_2N^{R'}_2)_2]^{2+}$ does not lead to observation of either a dihydrogen complex or a nickel dihydride complex. Both are rare for nickel, but dihydrogen complexes[57], and a nickel dihydride was observed at low temperature.[58] Instead of observing either a dihydrogen complex or dihydride of nickel, addition of H_2 to a solution of $[Ni(P^{Cy}_2N^{Bn}_2)_2]^{2+}$ (Cy = cyclohexyl, Bn = benzyl) produces three isomers of $[Ni(P^{Cy}_2N^{Bn}_2H)_2]^{2+}$, as shown in Scheme 5. The identities of these three isomers were established by NMR spectroscopic

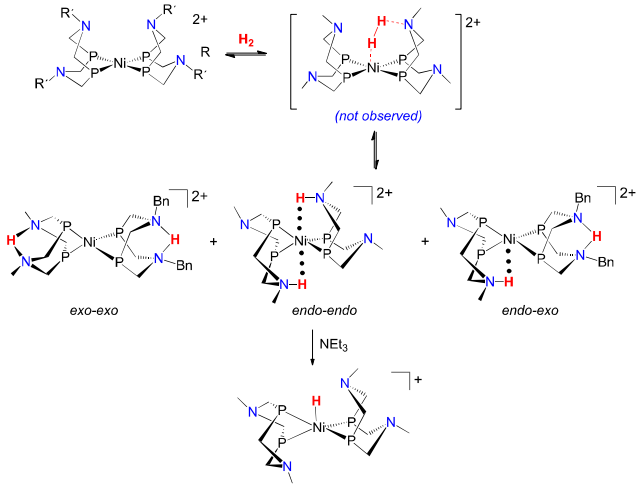

Scheme 5. Reaction of $[Ni(P^R_2N^{R'}_2)_2]^{2+}$ with H_2 to produce three isomers of the Ni(0) complex.

studies at low temperature, including the use of ^{15}N and deuterium labels.[59] Thus addition of H_2 leads to reduction of the Ni(II) center in $[Ni(P^{Cy}_2N^{Bn}_2)_2]^{2+}$ by two electrons, and the two protons are bound to different pendant amines in the ligands in the Ni(0) product. For the closely related complex with *tert*-butyl groups on the pendant amine, even when the addition of H_2 to $[Ni(P^{Cy}_2N^{t\text{-}Bu}_2)_2]^{2+}$ was carried out at -100 °C, no evidence was obtained for the putative dihydrogen complex $[Ni(\eta^2\text{-}H_2)(P^{Cy}_2N^{t\text{-}Bu}_2)_2]^{2+}$; the initial product observed at low temperature is the endo-endo isomer.[60]

A computational study using metadynamics simulations found evidence for the formation of a $[Ni(\eta^2\text{-}H_2)(P^{Cy}_2N^{Me}_2)_2]^{2+}$.[61] The binding of H_2 to the nickel center requires crossing a free energy

barrier of about 7-9 kcal/mol. The major contributor to the free energy barrier is loss of translational entropy of H_2. The computed activation barrier for heterolytic cleavage of H_2 bound to the Ni is about 5 kcal/mol, so this very low barrier is consistent with our inability to spectroscopically observe this complex.

In the experimental study, as solutions of $[Ni(P^{Cy}_2N^{Bn}_2H)_2]^{2+}$ are warmed, the kinetic product is converted to a mixture containing the endo-exo isomer and the exo-exo isomer. Measurements of the pK_a values in MeCN showed that the acidity of the three isomers are nearly the same, ranging from 13.2 – 13.5.[62] Addition of NEt_3 (pK_a of H-NEt_3^+ is 18.82)[27c] irreversibly deprotonates all three isomers, leading to the nickel hydride $[HNi(P^{Cy}_2N^{Bn}_2)_2]^+$.[62] Thus removal of one proton leads to migration of the other proton to the metal.

Intramolecular[63] and intermolecular proton mobility was studied in detail for isomers of $[Ni(P^{Cy}_2N^{Bn}_2H)_2]^{2+}$.[64] In the absence of any added base, solutions of the endo-endo isomer of $[Ni(P^{Cy}_2N^{Bn}_2H)_2]^{2+}$ initially isomerize to the endo-exo isomer, but the isomerization is slow, taking several hours at room temperature. Formation of the exo-exo isomer is even slower, taking more than two days to reach equilibrium. The equilibrium amounts of isomers of $[Ni(P^{Cy}_2N^{Bn}_2H)_2]^{2+}$ are 57% endo-exo, 30% endo-endo, and 13% exo-exo. The rate of approach to equilibrium between the three isomers is accelerated by a aniline (pK_a = 10.62 for anilinium).[27c] Aniline *reversibly* deprotonates $[Ni(P^{Cy}_2N^{Bn}_2H)_2]^{2+}$, leading to the hydride $[HNi(P^{Cy}_2N^{Bn}_2)_2]^+$, which is then re-protonated.

Computational studies using *ab initio* molecular dynamics provided insight into details of the intermolecular deprotonation/re-protonation process that leads to isomerization of the doubly protonated Ni(0) complexes.[64] These studies revealed that anilinium forms a strong hydrogen bonding interaction with the pendant amine, and breaking this N-H-N hydrogen bond contributes significantly to the barrier. The key role of theory and computations to understanding these reactions was recently reviewed.[65]

As shown in Scheme 5, both of the N-H bonds of $[Ni(P^{Cy}_2N^{Bn}_2H)_2]^{2+}$ engage in a hydrogen bonding interaction, for either positioning endo or exo. The N-H•••N hydrogen bond in the exo geometry is similar to those studied in detail for protonated 1,8-bis(dimethylamino)naphthalene[66] ("Proton Sponge®"). The N-H•••Ni hydrogen bond in the Ni(0) complex is a d(Ni)→σ*(N-H) interaction.[63] As described by Brammer[67] these interactions involve donation from a filled metal orbital into the σ* orbital of an N-H bond, and are classified as three-center, four-electron interactions. The N-H•••Ni and N-H•••N hydrogen bonds are of similar energy (7-9 kcal/mol), and therefore all three isomers of $[Ni(P^{Cy}_2N^{Bn}_2H)_2]^{2+}$ are of similar energy.

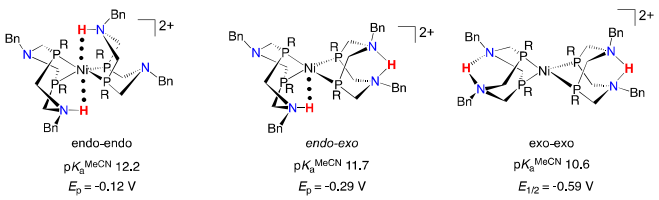

Fig. 5. pK_a and electrochemical data for the three isomers of the Ni(0) complex that result following addition of two protons and two electrons to $[Ni(P^{t\text{-}Bu}_2N^{Bn}_2H)_2]^{2+}$. The *tert*-Bu groups on P are not shown.

Electrochemical oxidation of Ni(0) to Ni(I) in $[Ni(P^{t\text{-}Bu}_2N^{Bn}_2H)_2]^{2+}$ shows that the exo-exo isomer of $[Ni(P^{t\text{-}Bu}_2N^{Bn}_2H)_2]^{2+}$ is easiest to oxidize, with $E_{1/2}$ = -0.59 V (vs. $Cp_2Fe^{+/0}$).[68] The N-H•••Ni interactions in the endo-exo and exo-exo isomers stabilize the Ni, shifting the Ni(I/0) potentials to more positive values as shown in Fig. 5. These electrochemical data provide estimates of 7.4 kcal/mol for the N-H•••Ni bond, and 3.7 kcal/mol for the second N-H•••Ni in the endo-endo isomer, giving an estimated total stabilization of the endo-endo isomer from hydrogen bonding of 11 kcal/mol. Oxidation of Ni(0) to Ni(I) likely leads to loss of the N-H•••Ni hydrogen bonding, which is expected to be much stronger in Ni(0) than in Ni(I) or Ni(II). Similar separations of the Ni(I/0) couples were found in $[Ni(P^{Cy}_2N^{t\text{-}Bu}_2H)_2]^{2+}$, with the potential for the endo-endo isomer (-0.36 V) being 120 mV positive of that for the endo-exo, and 530 mV positive of the potential for the exo-exo isomer.[60]

Thermodynamics for addition of H_2 to Ni(II) complexes

A key aspect of the rational design of metal catalysts (both thermal catalysts as well as electrocatalysts) is developing the ability to understand, and ultimately control, the thermodynamics for various bond forming and bond breaking reactions. Measurement of thermodynamic data can sometimes be tedious to carry out experimentally, but the resultant information is invaluable in guiding the rational design of catalysts. An ideal catalyst will convert the starting materials to products with a series of steps that avoid both high-energy and low-energy intermediates. Avoiding high energy intermediates may seem obvious, but low energy intermediates can be just as detrimental to fast catalysis, because of the activation barrier of the subsequent step, where the low-energy complex must be provided sufficient energy for the following step (Fig. 5).

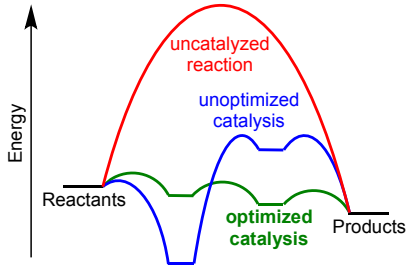

Fig. 6 Generalized scheme showing the energy for an uncatalyzed reaction, and unoptimized catalyst, and an optimized catalyst that has no high barriers or low energy intermediates.

Seeking to apply these concepts to the design of molecular electrocatalysts of nickel, the formation of the H-H bond occurs from the combination of the acidic N-H with the hydridic Ni-H bond, as implied in Fig. 4. The equations in Fig. 7 show that the driving force for formation/evolution of H_2 is greater when the N-H bond is more acidic and when the Ni-H bond is more hydridic, leading to the free energy for addition of H_2.

Thermochemical parameters (Table 2) show that the family of $[Ni(P^R_2N^{R'}_2)_2]^{2+}$ complexes span a range of about 21 kcal/mol in ΔG_{H2} as the R groups on P and the R´ groups on N are varied,

providing catalysts for H_2 production to H_2 oxidation.

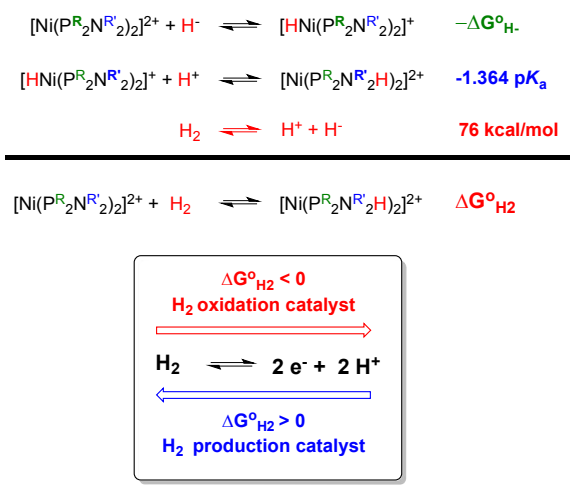

Fig. 7. Thermochemical cycle for determination of the free energy of addition of $_{H2}$

Table 2. Free Energy of Addition of H_2 to $[Ni(P^R{}_2N^{R'}{}_2)_2]^{2+}$ Complexes, thermodynamic hydricity of $[HNi(P^R{}_2N^{R'}{}_2)_2]^{+}$ and pK_a of the H_2 addition product $[Ni(P^R{}_2N^{R'}H)_2]^{2+}$.

Ni(II) complex	$\Delta G°_{H2}$ (kcal/mol)	$\Delta G°_{H-}$ (kcal/mol)	pK_a in MeCN	Ref
$[Ni(P^{Cy}{}_2N^{t\text{-}Bu}{}_2)_2]^{2+}$	-7.9	61.3	16.5	60
$[Ni(P^{Cy}{}_2N^{Bn}{}_2)_2]^{2+}$	-3.1	60.7	13.4	62
$[Ni(P^{Ph}{}_2N^{CH2CH2OMe}{}_2)_2]^{2+}$	+0.84	57.2	13.2	69
$[Ni(P^{Ph}{}_2N^{Bn}{}_2)_2]^{2+}$	+2.7	57.1	11.8	62
$[Ni(P^{Ph}{}_2N^{Ph}{}_2)_2]^{2+}$	+8.8	59.0	6.0	70
$[Ni(P^{n\text{-}Bu}{}_2N^{Ph}{}_2)_2]^{2+}$	+10.7	57.1	6.0	70
$[Ni(P^{Me}{}_2N^{Ph}{}_2)_2]^{2+}$	+13.8	54.0	6.0	71

Hydride donor abilities of metal hydrides can be measured by several methods.[31-32, 34, 36-37, 39-40, 42a, 42c, 43, 72] Heterolytic cleavage of H_2 with a base of appropriate strength is discussed above (Scheme 3). For Ni(diphosphine)$_2^{2+}$ complexes lacking pendant amines, a correlation has been determined between the Ni(II/I) couple and the hydride donor ability.[73] A similar correlation was also observed for the Ni(I/0) couple and the pK_a for the nickel hydride complexes, HNi^{II}(diphosphine)$_2^{2+}$. Analogous correlations have also been reported for $Ni(P^R{}_2N^{R'}{}_2)_2^{2+}$ complexes.[74] For either series of complexes, the nearly constant homolytic bond dissociation free energy results in a correlation between the respective redox couple and the corresponding heterolytic bond strength (hydride donor ability or pK_a value). As a result of this correlation, the Ni(II/I) and Ni(I/0) redox couples can be used to predict the acidity and hydricity of nickel hydride complexes HNi^{II}(diphosphine)$_2^{2+}$. As a validation and extension of these correlations, recent computational work has correlated these couples to additional thermochemical parameters for the Ni(diphosphine)$_2^{2+}$ complexes.[75]

Characterizing catalytic performance : measurement of turnover frequencies

The determination of catalytic rates is an essential step for the benchmarking and comparison of electrocatalysts. Due to the required proximity of a catalyst to an electrode surface for electrocatalysis to occur, in conjunction with the challenges of designing a well optimized electrolysis cell for any specific catalytic transformation (compatible with the required solvents, electrodes, acids, gases, and gas contacting), bulk electrolysis methods are not convenient for screening or characterizing the turnover frequency for new catalysts. A simple method for determining the TOF is highly desirable and is possible by comparing the observed current for a prospective catalyst under catalytic conditions to the current observed under non-catalytic conditions.[76] The general concept of current enhancement is illustrated in Figure 8, which shows data for production of H_2 catalyzed by $[Ni(P^{Ph}{}_2N^{Ph}{}_2)_2]^{2+}$.[77]

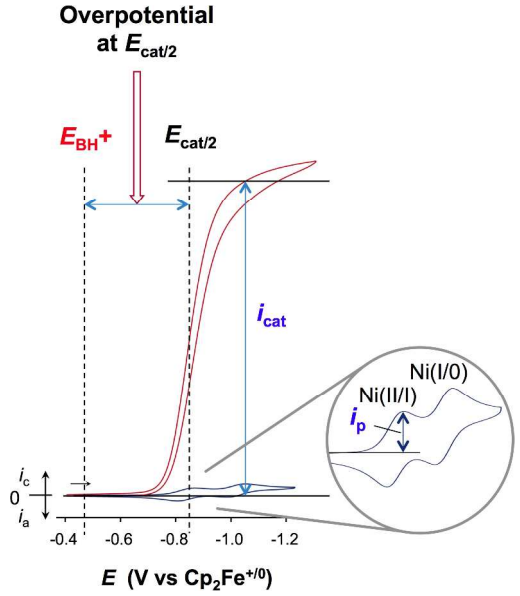

Fig. 8 Cyclic voltammogram of H_2 evolution catalysed by $[Ni(P^{Ph}{}_2N^{Ph}{}_2)_2]^{2+}$, showing catalytic current enhancement (difference between i_{cat} and i_p), thermodynamic potential for proton reduction (E_{BH}^{+}), $E_{cat/2}$ (half wave potential for catalysis), and the resultant overpotential at $E_{cat/2}$.

The catalytic current should generally be observed at a potential relevant to the molecular complex, such as the Ni(II/I) couple in the example shown in Figure 8. In some cases, the potentials may shift due to solution acidity (due to PCET or protonation that precedes reduction), thereby resulting in a catalytic wave that does not occur at the initially observed redox couples.[18c, 21a, 78]

The current enhancement (i_{cat}/i_p) illustrated in Figure 8 occurs at the Ni(II/I) couple in the example shown. This value of i_{cat}/i_p is related to the observed rate constant (k_{obs}) as shown in eq 7, and is essentially a measure of the rate of regeneration of the catalyst present in the diffusion layer.

$$\frac{i_{cat}}{i_p} = \frac{n}{0.4463}\sqrt{\frac{RTk_{obs}}{Fv}} \qquad (7)$$

Eq 7 applies to a one electron non-catalytic process (for i_p), and includes the universal gas constant (R), the temperature in Kelvin

(T), Faraday's Constant (F), and the scan rate (υ) in V/s. For a two-electron (n = 2) catalytic process at 25 °C, this equation simplifies (after rearrangement) to give k_{obs} (which is equal to the TOF) as shown in eq 8.

$$\mathrm{TOF} = 1.94 \cdot \upsilon \left(\frac{i_{cat}}{i_p}\right)^2 \qquad (8)$$

The accurate application of eqs 7 and 8 requires a significant current enhancement (greater than about 4), as well as careful determination that the observed catalytic process is at steady state, specifically that the catalytic wave is not diffusive and that the resulting TOF is independent of scan rate. While the catalytic current enhancement (i_{cat}/i_p) will vary with the scan rate, the overall TOF should be independent of the scan rate. It should be noted that eqs 7 and 8 yield a value for k_{obs} or TOF, which is not necessarily a simple rate constant, as it may be a pseudo first-order rate constant that is dependent upon the specific conditions. A recent example of this treatment has been reported for hydrogen production catalysts for which the current enhancement does not become independent of acid concentration.[79] As with all TOF values, the specific conditions should be reported (catalyst concentration, substrate concentrations or pressures, temperature, solvent, electrolyte, etc).

In addition to determining the catalytic rates, observation of the catalytic current as a function of catalyst concentration can provide mechanistic information. Specifically, the reaction order with respect to the catalyst concentration can be determined. For $[Ni(P^R{}_2N^{R'}{}_2)_2]^{2+}$ complexes, the studies to date have shown a first-order dependence on catalyst concentration.

Determination of overpotentials for molecular electrocatalysts

As illustrated in Figure 8, the overpotential for a molecular electrocatalyst for H_2 production is the difference between the thermodynamic potential for the reduction of an acid, BH^+, and the potential for the observed catalytic wave. The precise determination of each of these potentials is essential to accurately defining the reported overpotential for a catalyst. The determination of the thermodynamic potential will be discussed below. The definition of the catalytic potential requires a choosing a point on the catalytic wave that can be reliably and consistently determined. Because of the uncertainties in defining an onset potential at the base of the wave, the reporting of the catalytic potential at half of the observed current ($E_{cat/2}$, as shown in Figure 8) is preferred, as the greatest reproducibility will be obtained at the potential at which the current vs. potential trace has the highest slope. The difference between this potential and the thermodynamic potential defines the overpotential at $E_{cat/2}$.

Determining the thermodynamic potential for H^+/H_2

We and others had been using the method reported by Lichtenberger, Evans and co-workers[80] to estimate overpotential, which relies on the reported potential of standard state (1 M [H^+] and 1 atm H_2) hydrogen electrode in acetonitrile of -0.14 V vs $Cp_2Fe^{+/0}$. The potential of the H^+/H_2 couple has been debated for many years, with values ranging from -0.034 to -0.14 V. Due to the robust, extensive pK_a scale in MeCN, especially with the extensive work from Leito and co-workers on improving the self-consistency,[27a-d, 81] the potential of the H^+/H_2 couple was determined by measuring the equilibrium potentials (open circuit potentials) for buffered solutions using acid with known pK_a values and then extrapolating to standard state conditions.[77] Using this approach, the standard state potential for the H^+/H_2 couple was determined to be -0.028 vs $Cp_2Fe^{+/0}$, which is considerably more positive than many of the previous estimates. Correction of overpotentials determined using the previous H^+/H_2 potential of -0.14 V will result in larger reported overpotentials, by 0.11 V, but will improve the accuracy due to the increased consistency with the self-consistent pK_a scales in acetonitrile.

Beyond the determination of the potential for the H^+/H_2 couple, the use of this open circuit potential method allows the direct measurement of the thermodynamic potential for the conditions used for any specific catalytic studies. The overpotential can then be simply defined as the difference in potential between this thermodynamic potential and the potential at half of the catalytic current for any specific catalyst under the specific conditions used. This approach provides the ability to directly determine the thermodynamic potential for any specific acid or base in any solvent (or mixture of solvents), including solvents that are not typically used for thermodynamic studies, such as non-coordinating solvents like fluorobenzene[82] or novel solvents such as ionic liquids.[83]

A common complication for determination of overpotentials is the occurrence of homoconjugation. The self-association of an acid and the corresponding conjugate base can result in substantial deviations in the effective acidity or basicity, especially for carboxylic acids, which typically have high equilibrium constants for homoconjugation. Substantial deviations can result if homoconjugation is not avoided, or if the data is not corrected to account for influence of homoconjugation.[84] The use of acids with less extensive homoconjugation, or at lower concentrations, can help to minimize the effects of homoconjugation. For example, anilinium acids typically have much substantially smaller homoconjugation constants than carboxylic acids.

Evaluation of the effect of changing the basicity of the pendant amine in $[Ni(P^{Ph}{}_2N^{C6H4R}{}_2)_2]^{2+}$ electrocatalysts

A systematic study was carried out on reduction of protons by $[Ni(P^{Ph}{}_2N^{C6H4R}{}_2)_2](BF_4)_2$ complexes, where the substituent in the para position of the aromatic ring of the pendant amine was varied from electron-withdrawing groups (CF_3 and Br) to H (i.e., unsubstituted phenyl) to electron-donating groups (Me and OMe). This study provided an evaluation of the electrochemical data and catalytic rates while maintaining a constant steric environment around the Ni center. The $E_{1/2}$ values for this series of Ni(II) complexes showed a clear trend for both the Ni(II/I) and the Ni(I/0) couples. The potential of the Ni(II/I) couple varied from -0.74 V for R = CF_3 to -0.88 V for R = OMe. The trend is as expected, with the electron-donating OMe group leading to a more negative potential than the electron-withdrawing CF_3 substituent. It was surprising, however, that a change of 140 mV is observed from changing a substituent that is eight bonds removed from the metal. The Ni(I/0) couples exhibited a similar

trend, spanning a range of 180 mV, from -0.89 V for R = CF_3 to -1.07 V for R = OMe, revealing significant electronic communication through the P_2N_2 ligand to the nickel.

Electrocatalytic reduction of protons to produce H_2 used $[DMF(H)]^+OTf^-$. In dry acetonitrile solvent, the fastest turnover frequency (740 s^{-1} at 22 °C) was observed for $[Ni(P^{Ph}{}_2N^{C6H4Br}{}_2)_2]^{2+}$. Lower turnover frequencies were observed with R = H (590 s^{-1}) and R = OMe (310 s^{-1}). The II/I couple for R = OMe of -0.88 V is lower than that (-0.79 V) of the complex with R = Br (Fig. 9). This comparison illustrated an

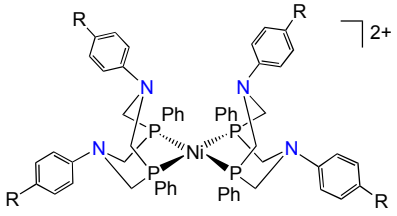

R = OMe, Me, H, $CH_2P(O)OEt_2$, Br, CF_3

$E_{1/2}$ Ni(II/I) = -0.88 V (vs. $Cp_2Fe^{+/0}$) for R = OMe
$E_{1/2}$ Ni(II/I) = -0.74 V (vs. $Cp_2Fe^{+/0}$) for R = CF_3

Fig. 9 $[Ni(P^{Ph}{}_2N^{C6H4R}{}_2)_2]^{2+}$ complexes studied as H_2 production electrocatalysts.

unusual trend of increasing turnover frequencies with more positive (i.e., less negative) potentials, showing that higher rates of catalysis can be achieved without increasing the overpotential. Considering the beneficial effect of the electron-withdrawing Br substituent, we expected that the complex with R = CF_3 would exhibit the fastest rate of catalysis, yet the opposite was observed, with the complex where R = CF_3 giving a TOF of only 95 s^{-1}. We believe this is due to removing too much electron density by the strongly electron-withdrawing CF_3 group. While the electron-withdrawing ability of Br is ideal in this case, the more electron-withdrawing CF_3 group apparently renders the pendant amine *insufficiently* basic, so that protonation is not complete following reduction of Ni(II) to Ni(I). The estimated[55] pK_a of 3.0 for the intermediate $[Ni(P^{Ph}{}_2N^{C6H4CF3}{}_2H)_2]^{2+}$ suggests that even with an excess of acid, that complete protonation by $[DMF(H)]^+$ would not occur, consistent with this interpretation. These results illustrate the importance of fine-tuning of the basicity of the pendant amine to achieve optimized rates of catalysis. Examples to be discussed later show that an alternative way to achieve "pK_a matching" is to change the pK_a of the acid to match that of the protonated pendant amine.

Sterics of the acid – bigger is not better

Electrocatalytic production of H_2 was also studied with this series of catalysts using anilinium acids, which are sterically bulkier than $[DMF(H)]^+$. Production of H_2 was studied using 2,6-dichloroanilinium (pK_a = 5.0 in MeCN)[27c] and *para*-cyanoanilinium (pK_a = 7.0 in MeCN)[85]. The turnover frequencies were all < 40 s^{-1} when using these anilinium acids. Since 2,6-dichloroanilinium is more acidic than $[DMF(H)]^+$ while *para*-cyanoanilinium is less acidic, the lower rates observed with both of these anilinium acids indicates a substantial decrease in rates as the size of the acid increased. Smaller acids are thus better able to deliver the proton to the catalytically active endo site of the catalyst.

Acceleration of H_2 production by water

Organometallic and inorganic chemists often fastidiously try to avoid traces of water, which can react with many metal complexes. We were surprised to find that addition of water can accelerate the rates of hydrogen production. For example, the turnover frequency of 590 s^{-1} using $[Ni(P^{Ph}{}_2N^{Ph}{}_2)_2]^{2+}$ as the catalyst increased to 720 s^{-1} when 0.03 M H_2O was added; similar accelerations of about 30-60% were observed upon addition of up to 0.55 M H_2O to other $[Ni(P^{Ph}{}_2N^{C6H4R}{}_2)_2]^{2+}$ catalysts.

This beneficial effect of water was discovered by accident. Puzzling results were obtained where different rates were found under ostensibly identical conditions until we ascertained that small amounts of water were influencing the rates. It is well-known that polar aprotic solvents such as MeCN are much more difficult to dry than non-polar solvents. Our experimental procedure for carrying out electrochemistry under rigorously dry conditions on the lab bench involves passing nitrogen over the solvent to avoid oxygen. Thus the N_2 should be dry, as well as the solvent and electrolyte. Moreover, the N_2 is typically bubbled through MeCN to saturate the N_2 with MeCN to avoid evaporating the solvent, which would change the concentrations of the catalyst and acid. Thus the MeCN in the bubbler also needs to be dry, along with any tubing to deliver the N_2 gas. After we confirmed that inadvertent changes in the concentration of water were the cause of the changes in observed rates, we found that reproducible rates were achievable for the catalytic reactions if adventitious water was excluded by conducting electrochemical studies under more rigorously dry conditions, such as in a glovebox. Using this approach, we can intentionally add carefully measured amounts of water to study the effect of water on catalysis.

Evaluation of the effect of changing the organic group on the diphosphine ligand in $[Ni(P^R{}_2N^{Ph}{}_2)_2]^{2+}$ electrocatalysts

A series of $[Ni(P^R{}_2N^{Ph}{}_2)_2]^{2+}$ catalysts was examined,[70-71] where the substituents on the P were varied, including methyl, *n*-butyl, Ph, CH_2CH_2Ph, benzyl, and 2,4,4-trimethylpentyl. As indicated by Fig. 10, variation of the organic group on P strongly influences the hydricity of the nickel hydride complexes, so the $\Delta G°_{H2}$ changes as well. The nickel hydride $[HNi(P^{Me}{}_2N^{Ph}{}_2)_2]^+$ ($\Delta G°_{H}$- = 54.0 kcal/mol), is a stronger hydride donor than $[HNi(P^{n\text{-}Bu}{}_2N^{Ph}{}_2)_2]^+$ ($\Delta G°_{H}$- = 57.1 kcal/mol) or $[HNi(P^{Bn}{}_2N^{Ph}{}_2)_2]^+$ ($\Delta G°_{H}$- = 59.4 kcal/mol). These differences in hydricity lead to more favorable free energies for release of H_2 (or less favorable free energy for H_2 addition) for the more hydridic Ni-H complexes, varying from $\Delta G°_{H2}$ = 13.8 kcal/mol for $[Ni(P^{Me}{}_2N^{Ph}{}_2)_2]^{2+}$ to 8.4 kcal/mol for $[Ni(P^{Bn}{}_2N^{Ph}{}_2)_2]^{2+}$. The turnover frequencies for the catalytic production of H_2 parallel the order of hydricity, with H_2 production catalyzed by $[Ni(P^{Me}{}_2N^{Ph}{}_2)_2]^{2+}$ in dry MeCN using $[DMF(H)]^+$ as the acid occurring at 1,540 s^{-1}. The thermodynamic driving force for

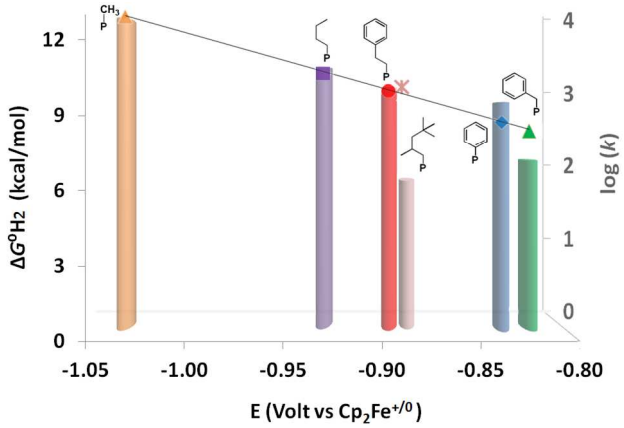

Fig. 10 Plot of free energy for elimination of H_2 vs the potential of the Ni(II/I) couple of $[Ni(P^R_2N^{Ph}_2)_2]^{2+}$, and a bar graph showing turnover frequencies.

H_2 production by $[Ni(P^{Bn}_2N^{Ph}_2)_2]^{2+}$ is much lower ($\Delta G°_{H2}$ = 8.4 kcal/mol), leading to a much lower TOF (7 s^{-1}). For these complexes the acceleration of the TOF for H_2 production in the presence of water was even greater than the series of $[Ni(P^{Ph}_2N^{C6H4R}_2)_2]^{2+}$ catalysts. For example, the TOF for H_2 production catalyzed by $[Ni(P^{n\text{-}Bu}_2N^{Ph}_2)_2]^{2+}$ increased from 46 s^{-1} in dry MeCN to 1820 s^{-1} with 3.4 M H_2O.

This series of $[Ni(P^R_2N^{Ph}_2)_2]^{2+}$ catalysts illustrates the changes in TOF as the hydride donor ability of the nickel hydride changes; since all of these complexes had Ph on the pendant amine, the basicity of the pendant amine (and hence acidity of the protonated amine) remained nearly constant. Fig. 9 shows the linear relationship between the free energy for addition/release of H_2 ($\Delta G°_{H2}$) and the $E_{½}$ of the Ni(II/I) couple. The bar graph in Fig. 9 shows that the TOFs observed are substantially influenced by the steric bulk of the substituent on P. The complexes with benzyl or 2,4,4-trimethylpentyl, the two groups that have branching at the β-carbon, lead to slower catalysts than would be predicted based on the linear plot of ΔG_{H2} vs. E for the other catalysts. A key step is delivery of a proton to the endo position of the pendant amine. With sterically bulky groups on the phosphine, endo protonation of the nitrogen (which is in proximity to the phosphorus substituent in the tetrahedral Ni(I) complex) is hindered due to the proximity of the phosphorus substituent when the complex is in the tetrahedral Ni(I) oxidation state. Correspondingly, catalysis is slower. The larger acceleration by added water in these catalysts suggests that water leads to more facile delivery of protons to the endo site, thus leading to more facile formation of the catalytically active intermediate and faster turnover frequencies.

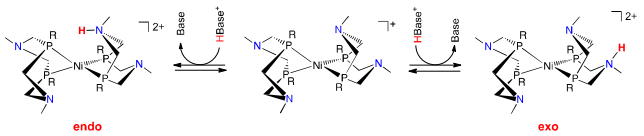

Scheme 6 Endo vs exo protonation of the Ni(I) complex that results from one-electron reduction of Ni(II)

Mechanism of production of H_2

The proposed mechanism for H_2 evolution from $[Ni(P^R_2N^{R'}_2)_2]^{2+}$ is shown in Fig. 11. Electrochemical reduction of Ni(II) to Ni(I) is followed by protonation of the pendant amine. This protonation is the key step that either leads to productive catalysis (when endo protonation occurs) or leads to protonation of the "wrong" isomer when the proton is delivered exo to the metal. The second electron transfer produces a Ni(0) complex with a protonated amine. Intramolecular proton transfer from the nitrogen to the nickel is followed by the second protonation to generate the key intermediate discussed earlier, which has the Ni-H bond and a N-H bond in close proximity. Fig. 11 shows the "dihydrogen bond"[86] between the protic N-H and hydridic Ni-H. Evolution of H_2 proceeds from this complex, regenerating the Ni(II) complex and completing the catalytic cycle.

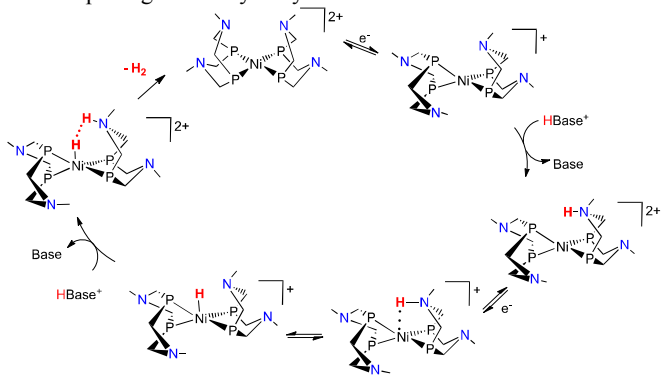

Fig. 11. Proposed mechanism for H_2 production catalysed by $[Ni(P^R_2N^{R'}_2)_2]^{2+}$. R groups on P are not shown, and R´ groups on N are not specified.

Change in mechanism: protonation prior to reduction

For H_2 production catalysts that contain more basic substituents at nitrogen, catalysis can occur either by the mechanism shown in Fig. 11, in which protonation occurs after reduction, or by initial protonation and subsequent reduction. For $[Ni(P^{Ph}_2N^{Bn}_2)_2]^{2+}$, the potential for the catalytic wave shifts from the Ni(II/I) couple to as much as 440 mV positive of the Ni(II/I) couple, with the shift in potential being dependent upon the strength of the acid used.[78] For the strongest acid used in this study, protonation appeared to occur prior to reduction. For weaker acids (higher pK_a values), a shift of 57 mV/pK_a unit for the catalytic wave was observed for this catalyst, consistent with a proton-coupled electron transfer (PCET) process for the reduction and protonation steps. This shift in potential with acid strength resulted in a nearly constant overpotential for evolution of H_2 by $[Ni(P^{Ph}_2N^{Bn}_2)_2]^{2+}$. Subsequent computational studies yielded results consistent with the proposed PCET process.[87]

A bi-directional catalyst for production and oxidation of H_2

One of the many remarkable features of hydrogenase enzymes[2a, 2c, 2d, 88] is that they catalyze both the oxidation of H_2 and the reverse, production of H_2. The ability to catalyze the reaction in both directions generally implies that the overpotential must be relatively small (less than 100 - 150 mV) for the catalysis by hydrogenases. By tuning the thermodynamics of H_2 addition to Ni(II) complexes, we have found a few catalysts for which the

addition of H_2 is nearly thermoneutral, and which can catalyze the reaction in both directions, providing synthetic catalysts that mimic that function of hydrogenase enzymes. The Ni(II) complex $[Ni(P^{Ph}_2N^{CH2CH2OMe}_2)_2]^{2+}$, with CH_2CH_2OMe substituents on the pendant amine, reacts reversibly with H_2 (K_{eq} = 0.24 atm-1 at 23 °C under 1 atm H_2) to give a mixture of the three isomers (cf. Scheme 5 and Fig. 5). When the acid p-cyanoanilinium is added to solutions of $[Ni(P^{Ph}_2N^{CH2CH2OMe}_2)_2]^{2+}$ enhanced current is observed at -0.55 V, indicating catalytic production of H_2. The Ni(II/I) couple of $[Ni(P^{Ph}_2N^{CH2CH2OMe}_2)_2]^{2+}$+ appears at -0.94 V, so the catalytic wave appears at a potential that is more than 300 mV less negative. A proton-coupled electron transfer is expected in this case, analogous to the proposed mechanism for $[Ni(P^{Ph}_2N^{Bn}_2)_2]^{2+}$ (discussed above), accounting for the catalytic wave occurring at a lower overpotential. The turnover frequency of the H_2 production catalysis is low (< 0.5 s^{-1}), however.

$[Ni(P^{Ph}_2N^{CH2CH2OMe}_2)_2]^{2+}$ was found to be a bi-directional catalyst, as it also catalyzes the oxidation of H_2, though also at a slow rate. When the reduction of protons is carried out under 1 atm H_2, the rate of production of H_2 is inhibited by the presence of H_2 (product inhibition), consistent with a catalyst that operates with a low overpotential.

Avoiding the N-H-N "pinch:" diphosphines with just one pendant amine

Extensive studies on the $[Ni(P^R_2N^{R'}_2)_2]^{2+}$ family of catalysts provided a good understanding of the factors governing catalytic rates, and how controlled movement of protons plays a key role in these electrocatalytic reactions. But these studies revealed a drawback to the $[Ni(P^R_2N^{R'}_2)_2]^{2+}$ systems, with the formation of exo-exo and endo-exo isomers being detrimental, since a significant amount of the Ni complexes is diverted into those unproductive isomers where the proton is "pinched" in a N-H-N hydrogen bond. Protonation of the Ni(0) complex $[Ni(P^{Cy}_2N^{t\text{-}Bu}_2)_2]$ by two equivalents of acid leads to the exo-exo isomer of $[Ni(P^{Cy}_2N^{t\text{-}Bu}_2H)_2]^{2+}$. Protonation at the endo site is needed for catalysis but is disfavored sterically. To avoid problems with the N-H-N "pinch" we prepared related catalysts that had just one, rather than two pendant amines in each diphosphine (eq. 9).

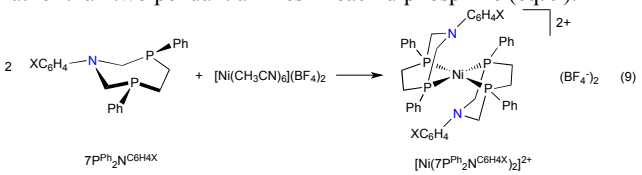

There are several differences in the Ni complexes with the $7P^{Ph}_2N^{Ph}$ ligand compared to the $[Ni(P^R_2N^{R'}_2)_2]^{2+}$ series of complexes. An x-ray crystal structure of $[Ni(7P^{Ph}_2N^{Ph})_2]^{2+}$ showed that the P-N-P bite angle was only 79.8°, compared to the 82-84° normally found in $[Ni(P^R_2N^{R'}_2)_2]^{2+}$ complexes. This change is largely the result of the 7-membered ring (vs. 8-membered ring in the $P^R_2N^{R'}_2$ ligand) which then leads to less steric interactions between Ph groups in $[Ni(7P^{Ph}_2N^{Ph})_2]^{2+}$. The crystal structure shows that all four P atoms and the Ni are in the same plane, whereas the crystal structure of $[Ni(P^{Ph}_2N^{C6H4Me}_2)_2]^{2+}$ showed a dihedral angle of 24 ° between the two planes containing the Ni and the two P atoms of the diphosphine. Whereas the Ni(II/I) and Ni(I/0) couples are usually well-separated in $[Ni(P^R_2N^{R'}_2)_2]^{2+}$ complexes, the cyclic voltammogram of $[Ni(7P^{Ph}_2N^{Ph})_2]^{2+}$ showed a wave at -1.13 V assigned as overlap of the two one-electron couples due to Ni(II/I) and Ni(I/0). The nickel hydride $[HNi(7P^{Ph}_2N^{Ph})_2]^+$ is estimated to have a thermodynamic hydricity of $\Delta G°_{H^-}$ = 54.9 kcal/mol,[79b] making it a substantially stronger hydride donor than $[HNi(P^{Ph}_2N^{Ph}_2)_2]^+$ ($\Delta G°_{H^-}$ = 59.0 kcal/mol). The high hydricity of $[HNi(7P^{Ph}_2N^{Ph})_2]^+$ contributes to the high driving force for H_2 production from these complexes, and the more negative potential for $[Ni(7P^{Ph}_2N^{Ph})_2]^{2+}$ leads to these complexes having a higher overpotential compared to related $[Ni(P^{Ph}_2N^{R'}_2)_2]^{2+}$ complexes.

Electrochemical reduction of solutions of $[Ni(7P^{Ph}_2N^{Ph})_2]^{2+}$ in the presence of $[DMF(H)]^+$ showed large increases in current, indicative of catalytic production of H_2 by reduction of protons. Ideally, a catalytic wave will exhibit a plateau shape, but at low scan rates, the waves exhibited waves that indicated diffusion control attributed to depletion of acid at the electrode caused by very fast catalysis. At a scan rate of 10V/s, however, the desired plateau shape was found, providing data that reliably indicated the turnover frequency for the catalytic reaction. The k_{obs} increases linearly with [acid], giving a turnover frequency of 33,000 s^{-1} at 0.43 M $[DMF(H)]^+$. With 1.2 M H_2O added, the ratio of i_{cat}/i_p was 74, which corresponds to a turnover frequency of 106,000 s^{-1}. This turnover frequency exceeds those reported for the [FeFe] hydrogenase enzyme, which is reported as 9,000 s^{-1} at 30 °C.[89] The very fast rate observed for this synthetic Ni catalyst shows that the ligand, and its positioned proton relays, support the intramolecular and intermolecular proton transfer steps required for the catalytic reaction, including the electron transfer (or proton-coupled electron transfer) steps.[90] Although this catalyst is exceptionally fast, it is not stable for long periods of time at higher acid concentrations, though all the kinetics were reported under conditions where less than 5% decomposition occurred. In addition, these catalysts have a high overpotential, whereas the natural hydrogenase enzymes are thought to operate at low overpotentials (< 100 mV).

The kinetics remain first-order in acid for H_2 production catalyzed by $[Ni(7P^{Ph}_2N^{Ph})_2]^{2+}$, in contrast to reactions catalyzed by $[Ni(P^{Ph}_2N^{Ph}_2)_2]^{2+}$, for which the reaction became zero-order in acid at high concentrations of acid. The mechanism is likely very similar for both classes of catalyst, despite the change in turnover-limiting step.

The effect of changing the substituent on the para position of the Ph ring on the N was examined for electron-donating groups (R = OMe and Me) and for electron-withdrawing substituents (R = Br, Cl and CF_3). In contrast to the $[Ni(P^R_2N^{R'}_2)_2]^{2+}$ complexes, where the catalytic reaction becomes independent of acid concentration at high acid concentrations, catalysis with $[Ni(7P^{Ph}_2N^{C6H4R})_2]^{2+}$ remains first-order in acid for all R groups except R = OMe, which begins to saturate at high concentrations of acid. Although two protons are required in the production of H_2, we have proposed that the turnover-limiting step is proton transfer to the Ni(I) complex $[Ni(7P^{Ph}_2N^{C6H4R})_2]^+$. We were initially surprised to find that electron-donating groups (R = OMe and Me) decreased the rate, *and* that electron-withdrawing groups also gave slower catalysts. In other words, the $[Ni(7P^{Ph}_2N^{Ph})_2]^{2+}$

catalyst that was synthesized first was the fastest, with changes in either direction of electron density at the aromatic ring leading to slower catalysis. This provided an example of the "principle of initial optimization!" The maximum TOF occurs near a pK_a value of 6.1, which is the pK_a of $[DMF(H)]^+$, the acid used in these experiments. The pK_a values of the endo protonated Ni(I) complexes $[Ni(7P^{Ph}_2N^{C6H4R}H)(7P^{Ph}_2N^{C6H4R})]^{2+}$ were calculated. Thus the fastest catalytic rate occurs when the pK_a of the added acid matches that of the protonated pendant amine of the Ni(I) complex. We believe that such matching of pK_a values will be important in the design of other catalysts, again emphasizing the need to control thermodynamics to avoid either high energy or low-energy intermediates.

The $7P_2N$ ligands avoid the problem of "pinching" of the N-H-N bonds, but for maximum catalytic activity, it remains critically important to achieve protonation at the endo site rather than the exo site (Scheme 7). When the pendant amine is more basic (e.g., R = OMe and Me) then the protonation at the "wrong" exo site is

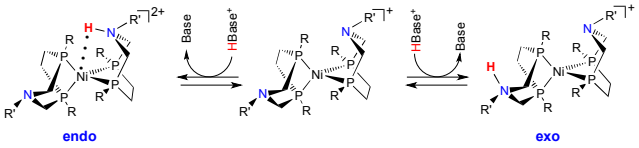

Scheme 7 Endo vs. exo protonation of the Ni(I) complex $[Ni(7P^{Ph}_2N^{Ph})_2]^+$.

more favorable, explaining why those catalysts are slower because of generation of larger amounts of the non-productive isomers. For the complexes with electron-withdrawing groups (R = Br, Cl and CF_3) on the N-aryl ring, the lower pK_a values for the protonated amines leads to the possibility that the proton transfer from the acid may be slow or incomplete, explaining the slower rates for those complexes.

Computational studies provided further insight into the energetics of protonation at endo vs. exo positions. Protonation of the endo site of $[Ni(7P^{Ph}_2N^{Ph})_2]^{2+}$ is favored by about 6 kcal/mol compared to protonation at the exo site.[79b] This preference is thought to be due to stabilization of the endo-protonated complex due to N-H•••Ni hydrogen bonding that is not possible to occur in the exo protonated isomer (Scheme 7). Note that the isomers shown in Scheme 7 are Ni(I) complexes that would have significantly weaker N-H•••Ni hydrogen bonding compared to those in Ni(0) complexes that form after the second electron and proton transfer (cf. Scheme 5 and Fig. 5). For the P_2N_2 complexes, the exo protonated Ni(I) complex $[Ni(P^R_2N^{R'}_2H)(P^R_2N^{R'}_2)]^{2+}$ is stabilized by N-H•••N hydrogen bonding that cannot occur in the complexes derived from $[Ni(7P^{Ph}_2N^{Ph})_2]^{2+}$. As a consequence, the two isomers are of nearly equal energy for the P_2N_2 complexes, since *both* sites of protonation lead to stabilization by hydrogen bonding.

In a comparison of three closely related Ni(II) complexes, a recent report highlights how changes to ligand structure can influence the thermodynamic preferences for proton delivery and hence, rates of catalysis.[91] The synthesis and electrochemical analysis of the $[Ni(8P_2N)_2]^{2+}$ complex provided a comparison of ligand structural effects and number of pendant amines on the rates of H_2 production to the $[Ni(7P_2N)_2]^{2+}$ and $[Ni(P_2N_2)_2]^{2+}$ complexes. The results of this study clearly indicate that the number of pendant amines and their basicity play a crucial role in the rate of delivery of protons to the metal center. The thermodynamic preference for formation of endo vs. exo protonation isomers increases from $[Ni(P_2N_2)_2]^{2+}$ to $[Ni(8P_2N)_2]^{2+}$ to $[Ni(7P_2N)_2]^{2+}$. As a result, a corresponding increase in the rate of H_2 production catalysis is observed in the same order. The

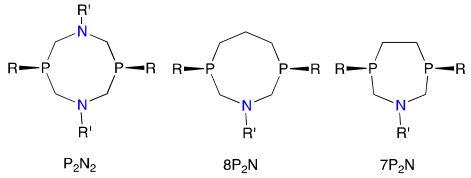

Chart 1. P_2N_2, $8P_2N$ and $7P_2N$ ligands.

data indicate that a large difference in the pK_a values for controlling proton delivery to endo over exo positions is an important feature for achieving fast catalytic rates. Even though the presence of only one pendant amine in the $8P_2N$ ligand precludes the formation of the N-H-N "pinch" that occurs in the $[Ni(P_2N_2)_2]^{2+}$ complexes, favoring protonation at the endo over exo position is still required for obtaining fast rates of catalysis.

Catalysis in an aqueous ionic liquid

Along with incorporation of pendant amines in ligands to function as proton relays, recent work has shown that catalysis can be accelerated by changing the medium, in cases where the solvent can play a direct role in the proton transfer process.[83] Dibutylformamidium bis(trifluoromethanesulfonyl)amide ([(DBF)H]NTf_2 (Fig. 12) is a protic ionic liquid that is readily prepared by protonation of dibutylformamide by $HNTf_2$. This acid is similar to the $[DMF(H)]^+$ used in many of our studies, but it is a liquid, whereas pure $[DMF(H)]^+OTf^-$ is a crystalline solid.

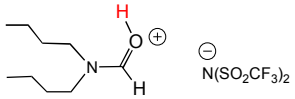

Fig. 12 A protic ionic liquid prepared by protonation of dibutylformamide

When mixed with water, the aqueous ionic liquid medium leads to fast catalysis in some cases. These experiments are conducted under somewhat different conditions than the typical experiments in MeCN solvent. Because of the concentration of ions in the ionic liquid medium, no additional electrolyte was required. Additionally, since the ionic liquid was a protic ionic liquid, no additional acid was required. Production of H_2 catalyzed by $[Ni(P^{Ph}_2N^{Ph}_2)_2]^{2+}$ in [(DBF)H]NTf_2 containing 72 mole% water gave a TOF of at least 5,500 s^{-1}, a substantial increase over the TOF of 720 s^{-1} found for the same catalyst using $[DMF(H)]^+$ with added water. An even greater enhancement of the TOF using [(DBF)H]NTf_2 containing 72 mole % water was found the related complex shown in Fig. 13 that has a hexyl group on the para position of each aryl ring bound to the pendant amine. The TOF for this complex in the aqueous protic ionic liquid was at least 43,000 s^{-1}, which is more than 50 times faster than was found in MeCN solvent using $[DMF(H)]^+$ with added water.

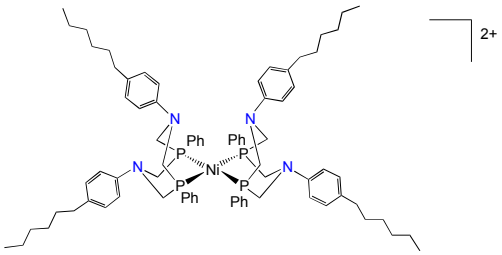

Fig. 13 $[Ni(P^{Ph}{}_2N^{C6H4(hexyl)}{}_2)_2]^{2+}$ catalyst

For other $[Ni(P^{Ph}{}_2N^{C6H4R}{}_2)_2]^{2+}$ complexes, however, the TOF was similar in MeCN compared to the protic ionic liquid/water medium, or even slower. Overall, the turnover frequencies increase with the hydrophobicity of the organic group on the arene, with the hexyl group giving the fastest rates. Further studies are underway in an attempt to understand and explain these effects more thoroughly. The results obtained so far do make it clear that control of proton delivery, and concomitant improvement of catalytic activity, can be improved by the solvent medium, in addition to the second coordination sphere effects provided by the pendant amines.

Rate accelerations in water-acetonitrile solutions

Most of the reactions discussed here have been carried out in acetonitrile, but recent work has explored Ni(II) complexes that have phenol groups on the pendant amine that enhance solubility of the complex in water. The Ni complex $[Ni(P^{Ph}{}_2N^{C6H4OH}{}_2)_2]^{2+}$ is not an especially good catalyst in MeCN.[92] Using $[DMF(H)]^+$ as the acid in anhydrous MeCN, the highest TOF observed for H_2 production was 35 s^{-1}. This complex dissolves in water/acetonitrile solutions containing up to about 75% water and provides superior performance in that medium. The TOF for H_2 production increases with acid concentrations from low acid concentrations up to about 2.8 M $HClO_4$. At that acid concentration, an $i_{cat}/i_p = 95$ was observed at a scan rate of $\upsilon = 10$ V s^{-1}, corresponding to a TOF of 170,000 s^{-1} at 25 °C.[92] At higher [acid] the TOF decreases, but addition of base restores the catalytic current, indicating the decrease in TOF at higher acid is not due to decomposition of the catalyst. In this example, as with the $[Ni(7P^{Ph}{}_2N^{C6H4R}{}_2)_2]^{2+}$ complexes discussed above, there is an optimum acid concentration for maximum catalytic activity. These experiments show a remarkably large effect of the aqueous medium on the catalytic activity. We believe the fast catalysis is due to the ability of H_3O^+ as the proton source in the aqueous acetonitrile medium to deliver protons to the endo position rather than diverting the catalyst into the non-productive exo-protonated isomer. The maximum TOF appears to occur when the pH of the medium matches that of the protonated Ni(I) complex, again demonstrating that controlling and directing proton delivery to the endo position is required for fast catalysis in these complexes. The overpotentials (directly experimentally measured[77]) at $E_{cat/2}$ varied from 310 mV (TOF = 750 s^{-1}) to 470 mV at the fastest TOF of 170,000 s^{-1}.

Conclusions and Outlook

Studies of the reactivity of metal hydrides, particularly when coupled with systematic thermochemical measurements and investigations of kinetics, have led to the ability to predict and control hydride transfer and proton transfer reactions of metal hydrides. Rational design of molecular electrocatalysts for production of H_2 by reduction of protons is facilitated greatly by thermochemical studies that reveal the free energy for elimination of H_2. Fast catalysts for H_2 production have been obtained when the free energy of H_2 *elimination* is favourable; conversely, catalysts for the oxidation of H_2 are obtained when the free energy for H_2 *addition* is thermodynamically favoured. Our studies focus on the role of pendant amines as proton relays that lower the barriers and overpotentials for catalytic evolution of H_2. The maximum benefit from pendant amines is obtained only when the basicity of the pendant amine is thermodynamically matched to the acid ("pK_a matching"). Positioning of the pendant amine is important so that the N-H resulting from protonation of the pendant amine is correctly positioned to interact with the M-H hydride, to lead to heterocoupling of protons and hydrides. The primary emphasis discussed here relates to nickel electrocatalysts for evolution of H_2, but it is important to recognize that these principles are applicable to a wide range of reactions of importance to energy conversions. We have shown that cobalt complexes with P_2N_2 ligands catalyse the evolution of H_2[93]. Iron complexes with P_2N_2 ligands lead to electrocatalysts for oxidation of H_2,[82, 94] and recent results from Sun and co-workers show the key role of a pendant amine in the oxidation of H_2 by a Fe_2 complex that is a model for the [FeFe]-hydrogenase.[95] A Mn complex with a P_2N_2 ligand gives extremely rapid, reversible heterolytic cleavage of H_2.[96] The principles discussed here for the two-proton, two-electron evolution of H_2 can be applied to the more complicated four-proton, four-electron reduction of oxygen. Mayer and co-workers have shown that CO_2H groups incorporated into an iron porphyrin leads to fast catalysis for reduction of O_2 to water,[97] and related catalysts with pyridine groups have also been reported recently.[98] Nocera and co-workers found cobalt complexes with "hangman" CO_2H groups are catalysts for reduction of O_2.[99] Recent efforts are exploring these principles to the six-proton, six-electron reduction of N_2.[100]

Acknowledgments

The research was supported as part of the Center for Molecular Electrocatalysis, an Energy Frontier Research Center funded by the U.S. Department of Energy, Office of Science, Office of Basic Energy Sciences. Pacific Northwest National Laboratory is operated by Battelle for DOE. We thank our colleagues who contributed to the work reviewed here.

Notes and references

[a] *Center for Molecular Electrocatalysis (efrc.pnnl.gov), Physical Sciences Division, Pacific Northwest National Laboratory, P.O. Box 999, K2-57. Tel: 509-372-6589; E-mail: morris.bullock@pnnl.gov*

† Electronic Supplementary Information (ESI) available: [none for this Feature Article]. See DOI: 10.1039/b000000x/

‡ In Scheme 3 and Fig. 6, the value of –1.364 log$K$ arises from (–RT ln K) converted to kcal/mol at 298 K and corrected from ln to log base 10 by dividing by log(e).

1. (a) N. S. Lewis and D. G. Nocera, *Proc. Natl. Acad. Sci. U.S.A.*, 2006, **103**, 15729-15735; (b) T. R. Cook, D. K. Dogutan, S. Y. Reece, Y. Surendranath, T. S. Teets and D. G. Nocera, *Chem. Rev.*, 2010, **110**, 6474-6502; (c) P. D. Tran, V. Artero and M. Fontecave, *Energy Environ. Sci.*, 2010, **3**, 727-747.
2. (a) J. C. Fontecilla-Camps, A. Volbeda, C. Cavazza and Y. Nicolet, *Chem. Rev.*, 2007, **107**, 4273-4303; (b) C. Tard and C. J. Pickett, *Chem. Rev.*, 2009, **109**, 2245-2274; (c) K. A. Vincent, A. Parkin and F. A. Armstrong, *Chem. Rev.*, 2007, **107**, 4366-4413; (d) J. A. Cracknell, K. A. Vincent and F. A. Armstrong, *Chem. Rev.*, 2008, **108**, 2439-2461.
3. (a) J. A. Wright, P. J. Turrell and C. J. Pickett, *Organometallics*, 2010, **29**, 6146-6156; (b) D. Chen, R. Scopelliti and X. Hu, *J. Am. Chem. Soc.*, 2009, **132**, 928-929; (c) D. Chen, R. Scopelliti and X. Hu, *Angew. Chem., Intl. Ed.*, 2010, **49**, 7512-7515.
4. (a) Y. Nicolet, C. Piras, P. Legrand, C. E. Hatchikian and J. C. Fontecilla-Camps, *Structure*, 1999, **7**, 13–23; (b) Y. Nicolet, A. L. de Lacey, X. Vernède, V. M. Fernandez, E. C. Hatchikian and J. C. Fontecilla-Camps, *J. Am. Chem. Soc.*, 2001, **123**, 1596-1601.
5. P. Knörzer, A. Silakov, C. E. Foster, F. A. Armstrong, W. Lubitz and T. Happe, *J. Biol. Chem.*, 2012, **287**, 1489-1499.
6. (a) A. Silakov, B. Wenk, E. Reijerse and W. Lubitz, *Phys. Chem. Chem. Phys.*, 2009, **11**, 6592–6599; (b) G. Berggren, A. Adamska, C. Lambertz, T. R. Simmons, J. Esselborn, M. Atta, S. Gambarelli, J. M. Mouesca, E. Reijerse, W. Lubitz, T. Happe, V. Artero and M. Fontecave, *Nature*, 2013, **499**, 66-69; (c) Y. Nicolet and J. C. Fontecilla-Camps, *J. Biol. Chem.*, 2012, **287**, 13532-13540.
7. (a) D. J. Evans and C. J. Pickett, *Chem. Soc. Rev.*, 2003, **32**, 268-275; (b) X. Liu, S. K. Ibrahim, C. Tard and C. J. Pickett, *Coord. Chem. Rev.*, 2005, **249**, 1641–1652; (c) Y. Wang, M. Wang, L. Sun and M. S. G. Ahlquist, *Chem. Commun.*, 2012, **48**, 4450-4452; (d) N. Wang, M. Wang, J. Liu, K. Jin, L. Chen and L. Sun, *Inorg. Chem.*, 2009, **48**, 11551-11558; (e) G. A. N. Felton, A. K. Vannucci, J. Chen, L. T. Lockett, N. Okumura, B. J. Petro, U. I. Zakai, D. H. Evans, R. S. Glass and D. L. Lichtenberger, *J. Am. Chem. Soc.*, 2007, **129**, 12521-12530; (f) G. A. N. Felton, A. K. Vannucci, N. Okumura, L. T. Lockett, D. H. Evans, R. S. Glass and D. L. Lichtenberger, *Organometallics*, 2008, **27**, 4671-4679; (g) M. K. Harb, U.-P. Apfel, J. Kübel, H. Görls, G. A. N. Felton, T. Sakamoto, D. H. Evans, R. S. Glass, D. L. Lichtenberger, M. El-khateeb and W. Weigand, *Organometallics*, 2009, **28**, 6666-6675; (h) J.-F. Capon, F. Gloaguen, P. Schollhammer and J. Talarmin, *Coord. Chem. Rev.*, 2005, **249**, 1664-1676; (i) J.-F. Capon, F. Gloaguen, P. Schollhammer and J. Talarmin, *J. Electroanal. Chem.*, 2006, **595**, 47-52; (j) J. F. Capon, S. Ezzaher, F. Gloaguen, F. Pétillon, P. Schollhammer and J. Talarmin, *Chem. Eur. J.*, 2008, **14**, 1954-1964; (k) J. F. Capon, F. Gloaguen, F. Y. Pétillon, P. Schollhammer and J. Talarmin, *Eur. J. Inorg. Chem.*, 2008, **2008**, 4671-4681; (l) P. Das, J.-F. Capon, F. Gloaguen, F. Y. Petillon, P. Schollhammer and J. Talarmin, *Inorg. Chem.*, 2004, **43**, 8203-8205; (m) S. Lounissi, G. Zampella, J. F. Capon, L. De Gioia, F. Matoussi, S. Mahfoudhi, F. Y. Petillon, P. Schollhammer and J. Talarmin, *Chem. Eur. J.*, 2012, **18**, 11123-11138; (n) D. Morvan, J. F. Capon, F. Gloaguen, A. LeGoff, M. Marchivie, F. Michaud, P. Schollhammer, J. Talarmin, J. J. Yaouanc, R. Pichon and N. Kervarec, *Organometallics*, 2007, **26**, 2042-2052; (o) M.-H. Chiang, Y.-C. Liu, S.-T. Yang and G.-H. Lee, *Inorg. Chem.*, 2009, **48**, 7604-7612; (p) Y.-C. Liu, T.-H. Yen, Y.-J. Tseng, C.-H. Hu, G.-H. Lee and M.-H. Chiang, *Inorg. Chem.*, 2012, **51**, 5997-5999; (q) Y.-C. Liu, K.-T. Chu, R.-L. Jhang, G.-H. Lee and M.-H. Chiang, *Chem. Commun.*, 2013, **49**, 4743-4745; (r) I. Aguirre de Carcer, A. DiPasquale, A. L. Rheingold and D. M. Heinekey, *Inorg. Chem.*, 2006, **45**, 8000-8002; (s) S. L. Matthews and D. M. Heinekey, *Inorg. Chem.*, 2010, **49**, 9746-9748; (t) S. L. Matthews and D. M. Heinekey, *Inorg. Chem.*, 2011, **50**, 7925-7927; (u) S. Ott, M. Kritikos, B. Åkermark, L. Sun and R. Lomoth, *Angew. Chem., Int. Ed.*, 2004, **43**, 1006-1009; (v) L. Schwartz, G. Eilers, L. Eriksson, A. Gogoll, R. Lomoth and S. Ott, *Chem. Commun.*, 2006, 520-522; (w) L. Schwartz, J. Ekström, R. Lomoth and S. Ott, *Chem. Commun.*, 2006, 4206-4208; (x) G. Eilers, L. Schwartz, M. Stein, G. Zampella, L. de Gioia, S. Ott and R. Lomoth, *Chem. Eur. J.*, 2007, **13**, 7075-7084; (y) R. Lomoth and S. Ott, *Dalton Trans.*, 2009, 9952-9959; (z) P. S. Singh, H. C. Rudbeck, P. Huang, S. Ezzaher, L. Eriksson, M. Stein, S. Ott and R. Lomoth, *Inorg. Chem.*, 2009, **48**, 10883-10885; (aa) S. Kaur-Ghumaan, L. Schwartz, R. Lomoth, M. Stein and S. Ott, *Angew. Chem., Int. Ed.*, 2010, **49**, 8033-8036.
8. C. Tard, X. Liu, S. K. Ibrahim, M. Bruschi, L. D. Gioia, S. Davies, X. Yang, L.-S. Wang, G. Sawers and C. J. Pickett, *Nature*, 2005, **434**, 610-613.
9. (a) J. D. Lawrence, H. Li, T. B. Rauchfuss, M. Bénard and M.-M. Rohme, *Angew. Chem., Int. Ed.*, 2001, **40**, 1768-1771; (b) F. Gloaguen, J. D. Lawrence, T. B. Rauchfuss, M. Benard and M.-M. Rohmer, *Inorg. Chem.*, 2002, **41**, 6573-6582; (c) A. K. Justice, T. B. Rauchfuss and S. R. Wilson, *Angew. Chem., Int. Ed.*, 2007, **46**, 6152-6154; (d) M. T. Olsen, T. B. Rauchfuss and S. R. Wilson, *J. Am. Chem. Soc.*, 2010, **132**, 17733-17740; (e) J. M. Camara and T. B. Rauchfuss, *J. Am. Chem. Soc.*, 2011, **133**, 8098-8101; (f) W. Wang, M. J. Nilges, T. B. Rauchfuss and M. Stein, *J. Am. Chem. Soc.*, 2013, **135**, 3633-3639.
10. (a) F. Gloaguen and T. B. Rauchfuss, *Chem. Soc. Rev.*, 2009, **38**, 100-108; (b) B. E. Barton and T. B. Rauchfuss, *Inorg. Chem.*, 2008, **47**, 2261-2263; (c) R. Zaffaroni, T. B. Rauchfuss, D. L. Gray, L. De Gioia and G. Zampella, *J. Am. Chem. Soc.*, 2012, **134**, 19260-19269.
11. M. E. Carroll, B. E. Barton, T. B. Rauchfuss and P. J. Carroll, *J. Am. Chem. Soc.*, 2012, **134**, 18843–18852.
12. J. M. Camara and T. B. Rauchfuss, *Nat. Chem.*, 2012, **4**, 26-30.
13. (a) E. J. Lyon, I. P. Georgakaki, J. H. Reibenspies and M. Y. Darensbourg, *Angew. Chem., Int. Ed.*, 1999, **38**, 3178-3180; (b) X. Zhao, I. P. Georgakaki, M. L. Miller, J. C. Yarbrough and M. Y. Darensbourg, *J. Am. Chem. Soc.*, 2001, **123**, 9710-9711; (c) X. Zhao, I. P. Georgakaki, M. L. Miller, R. Mejia-Rodriguez, C.-Y. Chiang and M. Y. Darensbourg, *Inorg. Chem.*, 2002, **41**, 3917-3928.

14. (a) D. Chong, I. P. Georgakaki, R. Mejia-Rodriguez, J. Sanabria-Chinchilla, M. P. Soriaga and M. Y. Darensbourg, *Dalton Trans.*, 2003, 4158-4163; (b) R. Mejia-Rodriguez, D. Chong, J. H. Reibenspies, M. P. Soriaga and M. Y. Darensbourg, *J. Am. Chem. Soc.*, 2004, **126**, 12004-12014; (c) P. Surawatanawong, J. W. Tye, M. Y. Darensbourg and M. B. Hall, *Dalton Transactions*, 2010, **39**, 3093-3104; (d) M. L. Singleton, D. J. Crouthers, R. P. Duttweiler, III, J. H. Reibenspies and M. Y. Darensbourg, *Inorg. Chem.*, 2011, **50**, 5015-5026.
15. (a) M. Y. Darensbourg, E. J. Lyon, X. Zhao and I. P. Georgakaki, *Proc. Natl. Acad. Sci. U.S.A.*, 2003, **100**, 3683-3688; (b) I. P. Georgakaki, L. M. Thomson, E. J. Lyon, M. B. Hall and M. Y. Darensbourg, *Coord. Chem. Rev.*, 2003, **238-239**, 255-266; (c) J. W. Tye, J. Lee, H.-W. Wang, R. Mejia-Rodriguez, J. H. Reibenspies, M. B. Hall and M. Y. Darensbourg, *Inorg. Chem.*, 2005, **44**, 5550-5552; (d) T. Liu and M. Y. Darensbourg, *J. Am. Chem. Soc.*, 2007, **129**, 7008-7009; (e) M. L. Singleton, N. Bhuvanesh, J. H. Reibenspies and M. Y. Darensbourg, *Angew. Chem., Int. Ed.*, 2008, **47**, 9492-9495.
16. (a) M. Rakowski DuBois and D. L. DuBois, *Chem. Soc. Rev.*, 2009, **38**, 62-72; (b) W. J. Shaw, M. L. Helm and D. L. DuBois, *Biochimica et Biophysica Acta (BBA) - Bioenergetics*, 2013, **1827**, 1123-1139.
17. (a) R. M. Bullock, ed., *Catalysis Without Precious Metals*, Wiley-VCH, Weinheim, 2010; (b) M. Wang, L. Chen and L. Sun, *Energy Environ. Sci.*, 2012, **5**, 6763-6778; (c) V. S. Thoi, Y. Sun, J. R. Long and C. J. Chang, *Chem. Soc. Rev.*, 2013, **42**, 2388-2400; (d) J. R. McKone, S. C. Marinescu, J. Winkler, B. S. Brunschwig and H. Gray, *Chemical Science*, 2013.
18. (a) A. Le Goff, V. Artero, B. Jousselme, P. D. Tran, N. Guillet, R. Métayé, A. Fihri, S. Palacin and Fontecave, *Science*, 2009, **326**, 1384-1387; (b) P. D. Tran, A. Le Goff, J. Heidkamp, B. Jousselme, N. Guillet, S. Palacin, H. Dau, M. Fontecave and V. Artero, *Angew. Chem. Int. Ed.*, 2011, **50**, 1371-1374; (c) P.-A. Jacques, V. Artero, J. Pécaut and M. Fontecave, *Proc. Natl. Acad. Sci. U.S.A.*, 2009, **106**, 20627-20632; (d) O. R. Luca, J. D. Blakemore, S. J. Konezny, J. M. Praetorius, T. J. Schmeier, G. B. Hunsinger, V. S. Batista, G. W. Brudvig, N. Hazari and R. H. Crabtree, *Inorg. Chem.*, 2012, **51**, 8704-8709.
19. M. J. Rose, H. B. Gray and J. R. Winkler, *J. Am. Chem. Soc.*, 2012, **134**, 8310-8313.
20. (a) X. Hu, B. S. Brunschwig and J. C. Peters, *J. Am. Chem. Soc.*, 2007, **129**, 8988-8998; (b) B. D. Stubbert, J. C. Peters and H. B. Gray, *J. Am. Chem. Soc.*, 2011, **133**, 18070-18073; (c) J. L. Dempsey, J. R. Winkler and H. B. Gray, *J. Am. Chem. Soc.*, 2010, **132**, 1060-1065; (d) J. L. Dempsey, B. S. Brunschwig, J. R. Winkler and H. B. Gray, *Acc. Chem. Res.*, 2009, **42**, 1995-2004; (e) J. L. Dempsey, J. R. Winkler and H. B. Gray, *J. Am. Chem. Soc.*, 2010, **132**, 16774-16776; (f) C. N. Valdez, J. L. Dempsey, B. S. Brunschwig, J. R. Winkler and H. B. Gray, *Proc. Natl. Acad. Sci. U.S.A.*, 2012, **109**, 15589-15593; (g) Y. Sun, J. P. Bigi, N. A. Piro, M. L. Tang, J. R. Long and C. J. Chang, *J. Am. Chem. Soc.*, 2011, **133**, 9212-9215; (h) Y. Sun, J. Sun, J. R. Long, P. Yang and C. J. Chang, *Chemical Science*, 2013, **4**, 118-124; (i) M. Razavet, V. Artero and M. Fontecave, *Inorg. Chem.*, 2005, **44**, 4786-4795; (j) C. Baffert, V. Artero and M. Fontecave, *Inorg. Chem.*, 2007, **46**, 1817-1824; (k) V. Artero and M. Fontecave, *Coord. Chem. Rev.*, 2005, **249**, 1518–1535.
21. (a) A. M. Appel, D. L. DuBois and M. Rakowski DuBois, *J. Am. Chem. Soc.*, 2005, **127**, 12717–12726; (b) H. I. Karunadasa, C. J. Chang and J. R. Long, *Nature*, 2010, **464**, 1329-1333; (c) H. I. Karunadasa, E. Montalvo, Y. Sun, M. Majda, J. R. Long and C. J. Chang, *Science*, 2012, **335**, 698-702; (d) E. J. Sundstrom, X. Yang, V. S. Thoi, H. I. Karunadasa, C. J. Chang, J. R. Long and M. Head-Gordon, *J. Am. Chem. Soc.*, 2012, **134**, 5233-5242.
22. H. D. Kaesz and R. B. Saillant, *Chem. Rev.*, 1972, **72**, 231-281.
23. (a) R. Bau, ed., *Transition Metal Hydrides*, American Chemical Society, Washington, D.C., 1978; (b) A. Dedieu, ed., *Transition Metal Hydrides*, VCH, New York, 1991.
24. (a) D. C. Eisenberg and J. R. Norton, *Isr. J. Chem.*, 1991, **31**, 55-66; (b) D. C. Eisenberg, C. J. C. Lawrie, A. E. Moody and J. R. Norton, *J. Am. Chem. Soc.*, 1991, **113**, 4888-4895.
25. (a) D. M. Smith, M. E. Pulling and J. R. Norton, *J. Am. Chem. Soc.*, 2007, **129**, 770-771; (b) J. Hartung, M. E. Pulling, D. M. Smith, D. X. Yang and J. R. Norton, *Tetrahedron*, 2008, **64**, 11822-11830.
26. (a) R. F. Jordan and J. R. Norton, *J. Am. Chem. Soc.*, 1982, **104**, 1255-1263; (b) E. J. Moore, J. M. Sullivan and J. R. Norton, *J. Am. Chem. Soc.*, 1986, **108**, 2257-2263; (c) R. T. Edidin, J. M. Sullivan and J. R. Norton, *J. Am. Chem. Soc.*, 1987, **109**, 3945-3953; (d) S. S. Kristjánsdóttir, A. E. Moody, R. T. Weberg and J. R. Norton, *Organometallics*, 1988, **7**, 1983-1987; (e) S. S. Kristjánsdóttir and J. R. Norton, in *Transition Metal Hydrides*, ed. A. Dedieu, VCH, New York, 1991 (Chapter 9), pp. 309-359.
27. (a) I. Leito, I. Kaljurand, I. A. Koppel, L. M. Yagupolskii and V. M. Vlasov, *J. Org. Chem.*, 1998, **63**, 7868-7874; (b) I. Kaljurand, T. Rodima, I. Leito, I. A. Koppel and R. Schwesinger, *J. Org. Chem.*, 2000, **65**, 6202-6208; (c) I. Kaljurand, A. Kutt, L. Soovali, T. Rodima, V. Maemets, I. Leito and I. A. Koppel, *J. Org. Chem.*, 2005, **70**, 1019-1028; (d) A. Kütt, I. Leito, I. Kaljurand, L. Soovali, V. M. Vlasov, L. M. Yagupolskii and I. A. Koppel, *J. Org. Chem.*, 2006, **71**, 2829-2838; (e) A. Kütt, T. Rodima, J. Saame, E. Raamat, V. Mäemets, I. Kaljurand, I. A. Koppel, R. Y. Garlyauskayte, Y. L. Yagupolskii, L. M. Yagupolskii, E. Bernhardt, H. Willner and I. Leito, *The Journal of Organic Chemistry*, 2011, **76**, 391-395.
28. J. A. S. Roberts, A. M. Appel, D. L. DuBois and R. M. Bullock, *J. Am. Chem. Soc.*, 2011, **133**, 14604-14613.
29. O. B. Ryan, M. Tilset and V. D. Parker, *J. Am. Chem. Soc.*, 1990, **112**, 2618-2626.
30. M. Tilset, *J. Am. Chem. Soc.*, 1992, **114**, 2740-2741.
31. R. Ciancanelli, B. C. Noll, D. L. DuBois and M. R. DuBois, *J. Am. Chem. Soc.*, 2002, 2984-2992.
32. D. E. Berning, B. C. Noll and D. L. DuBois, *J. Am. Chem. Soc.*, 1999, **121**, 11432-11447.
33. (a) J. M. Hanckel and M. Y. Darensbourg, *J. Am. Chem. Soc.*, 1983, **105**, 6979-6980; (b) M. Y. Darensbourg and M. M. Ludvig, *Inorg. Chem.*, 1986, **25**, 2894-2898.

34. C. J. Curtis, A. Miedaner, W. W. Ellis and D. L. DuBois, *J. Am. Chem. Soc.*, 2002, **124**, 1918-1925.
35. D. D. M. Wayner and V. D. Parker, *Acc. Chem. Res.*, 1993, **26**, 287-294.
36. M. T. Mock, R. G. Potter, D. M. Camaioni, J. Li, W. G. Dougherty, W. S. Kassel, B. Twamley and D. L. DuBois, *J. Am. Chem. Soc.*, 2009, **131**, 14454-14465.
37. W. W. Ellis, R. Ciancanelli, S. M. Miller, J. W. Raebiger, M. R. DuBois and D. L. DuBois, *J. Am. Chem. Soc.*, 2003, **125**, 12230-12236.
38. M. T. Mock, R. G. Potter, M. J. O'Hagan, D. M. Camaioni, W. G. Dougherty, W. S. Kassel and D. L. DuBois, *Inorg. Chem.*, 2011, **50**, 11914-11928.
39. W. W. Ellis, J. W. Raebiger, C. J. Curtis, J. W. Bruno and D. L. DuBois, *J. Am. Chem. Soc.*, 2004, **126**, 2738-2743.
40. A. Miedaner, J. W. Raebiger, C. J. Curtis, S. M. Miller and D. L. DuBois, *Organometallics*, 2004, **23**, 2670-2679.
41. J.-P. Cheng, K. L. Handoo and V. D. Parker, *J. Am. Chem. Soc.*, 1993, **115**, 2655-2660.
42. (a) A. J. Price, R. Ciancanelli, B. C. Noll, C. J. Curtis, D. L. DuBois and M. Rakowski DuBois, *Organometallics*, 2002, **21**, 4833-4839; (b) D. L. DuBois, D. M. Blake, A. Miedaner, C. J. Curtis, M. R. DuBois, J. A. Franz and J. C. Linehan, *Organometallics*, 2006, 4414-4419; (c) J. W. Raebiger and D. L. DuBois, *Organometallics*, 2005, **24**, 110-118.
43. J. W. Raebiger, A. Miedaner, C. J. Curtis, S. M. Miller, O. P. Anderson and D. L. DuBois, *J. Am. Chem. Soc.*, 2004, **126**, 5502-5514.
44. (a) X. J. Qi, Y. Fu, L. Liu and Q. X. Guo, *Organometallics*, 2007, **26**, 4197-4203; (b) M. R. Nimlos, C. H. Chang, C. J. Curtis, A. Miedaner, H. M. Pilath and D. L. DuBois, *Organometallics*, 2008, **27**, 2715-2722.
45. J. A. Labinger and K. H. Komadina, *J. Organomet. Chem.*, 1978, **155**, C25-C28.
46. M. Y. Darensbourg and C. E. Ash, *Adv. Organomet. Chem.*, 1987, **27**, 1-50.
47. S. C. Kao and M. Y. Darensbourg, *Organometallics*, 1984, **3**, 646-647.
48. S. C. Kao, P. L. Gaus, K. Youngdahl and M. Y. Darensbourg, *Organometallics*, 1984, **3**, 1601-1603.
49. P. L. Gaus, S. C. Kao, K. Youngdahl and M. Y. Darensbourg, *J. Am. Chem. Soc.*, 1985, **107**, 2428-2434.
50. S. C. Kao, C. T. Spillett, C. Ash, R. Lusk, Y. K. Park and M. Y. Darensbourg, *Organometallics*, 1985, **4**, 83-91.
51. (a) R. M. Bullock, in *Handbook of Homogeneous Hydrogenation*, eds. J. G. de Vries and C. J. Elsevier, Wiley-VCH, Weinheim, Germany, 2007, Chapter 7, pp. 153-197; (b) R. M. Bullock, *Chem. Eur. J.*, 2004, **10**, 2366-2374; (c) R. M. Bullock, in *Catalysis Without Precious Metals*, ed. R. M. Bullock, Wiley-VCH, Weinheim, 2010.
52. (a) J.-S. Song, D. J. Szalda, R. M. Bullock, C. J. C. Lawrie, M. A. Rodkin and J. R. Norton, *Angew. Chem., Int. Ed. Engl.*, 1992, **31**, 1233-1235; (b) R. M. Bullock and M. H. Voges, *J. Am. Chem. Soc.*, 2000, **122**, 12594-12595; (c) M. H. Voges and R. M. Bullock, *J. Chem. Soc., Dalton Trans.*, 2002, 759-770.
53. (a) T.-Y. Cheng, B. S. Brunschwig and R. M. Bullock, *J. Am. Chem. Soc.*, 1998, **120**, 13121-13137; (b) T.-Y. Cheng and R. M. Bullock, *J. Am. Chem. Soc.*, 1999, **121**, 3150-3155; (c) T.-Y. Cheng and R. M. Bullock, *Organometallics*, 2002, **21**, 2325-2331.
54. I. Faviera and E. Duñach, *Tetrahedron Letters*, 2004, **45**, 3393-3395.
55. U. Kilgore, J. Roberts, D. H. Pool, A. Appel, M. Stewart, M. Rakowski DuBois, W. G. Dougherty, W. S. Kassel, R. M. Bullock and D. L. DuBois, *J. Am. Chem. Soc.*, 2011, **133**, 5861-5872.
56. (a) G. J. Kubas, *Metal Dihydrogen and σ-Bond Complexes: Structure, Theory, and Reactivity*, Kluwer Academic/Plenum Publishers, New York, 2001; (b) G. J. Kubas, *Chem. Rev.*, 2007, **107**, 4152-4205; (c) D. M. Heinekey and W. J. Oldham, Jr., *Chem. Rev.*, 1993, **93**, 913-926.
57. (a) T. He, N. P. Tsvetkov, J. G. Andino, X. Gao, B. C. Fullmer and K. G. Caulton, *J. Am. Chem. Soc.*, 2010, **132**, 910-911; (b) C. Tsay and J. C. Peters, *Chemical Science*, 2012, **3**, 1313-1318; (c) S. J. Connelly, A. C. Zimmerman, W. Kaminsky and D. M. Heinekey, *Chemistry – A European Journal*, 2012, **18**, 15932-15934.
58. J. Y. Yang, R. M. Bullock, W. J. Shaw, B. Twamley, K. Fraze, M. Rakowski DuBois and D. L. DuBois, *J. Am. Chem. Soc.*, 2009, **131**, 5935–5945.
59. A. D. Wilson, R. K. Shoemaker, A. Miedaner, J. T. Muckerman, D. L. DuBois and M. Rakowski DuBois, *Proc. Natl. Acad. Sci. U.S.A.*, 2007, **104**, 6951-6956.
60. J. Y. Yang, S. E. Smith, T. Liu, W. G. Dougherty, W. A. Hoffert, W. S. Kassel, M. R. DuBois, D. L. DuBois and R. M. Bullock, *J. Am. Chem. Soc.*, 2013, **135**, 9700-9712.
61. S. Raugei, S. Chen, M. H. Ho, B. Ginovska-Pangovska, R. J. Rousseau, M. Dupuis, D. L. DuBois and R. M. Bullock, *Chem. Eur. J.*, 2012, **18**, 6493-6506.
62. K. Fraze, A. D. Wilson, A. M. Appel, M. Rakowski DuBois and D. L. DuBois, *Organometallics*, 2007, **26**, 3918-3924.
63. M. O'Hagan, W. J. Shaw, S. Raugei, S. Chen, J. Y. Yang, U. J. Kilgore, D. L. DuBois and R. M. Bullock, *J. Am. Chem. Soc.*, 2011, **133**, 14301-14312.
64. M. O'Hagan, M. H. Ho, J. Y. Yang, A. M. Appel, M. Rakowski DuBois, S. Raugei, W. J. Shaw, D. L. DuBois and R. M. Bullock, *J. Am. Chem. Soc.*, 2012, **134**, 19409-19424.
65. M.-H. Ho, S. Chen, R. Rousseau, M. Dupuis, R. M. Bullock and S. Raugei, in *Applications of Molecular Modeling to Challenges in Clean Energy*, American Chemical Society, 2013, pp. 89-111.
66. (a) F. Hibbert, *Acc. Chem. Res.*, 1984, **17**, 115-120; (b) R. W. Alder, *Chem. Rev.*, 1989, **89**, 1215-1223.
67. L. Brammer, *Dalton Trans.*, 2003, 3145-3157.
68. E. S. Wiedner, J. Y. Yang, S. Chen, S. Raugei, W. G. Dougherty, W. S. Kassel, M. L. Helm, R. M. Bullock, M. Rakowski DuBois and D. L. DuBois, *Organometallics*, 2012, **31**, 144-156.
69. S. E. Smith, J. Y. Yang, D. L. DuBois and R. M. Bullock, *Angew. Chem. Int. Ed.*, 2012, **51**, 3152-3155.
70. U. J. Kilgore, M. P. Stewart, M. L. Helm, W. G. Dougherty, W. S. Kassel, M. Rakowski DuBois, D. L. DuBois and R. M. Bullock, *Inorg. Chem.*, 2011, **50**, 10908–10918.

71. S. Wiese, U. J. Kilgore, D. L. DuBois and R. M. Bullock, *ACS Catalysis*, 2012, **2**, 720-727.
72. C. J. Curtis, A. Miedaner, J. W. Raebiger and D. L. DuBois, *Organometallics*, 2004, **23**, 511-516.
73. D. E. Berning, A. Miedaner, C. J. Curtis, B. C. Noll, M. C. Rakowski DuBois and D. L. DuBois, *Organometallics*, 2001, **20**, 1832-1839.
74. B. R. Galan, J. Schöffel, J. C. Linehan, C. Seu, A. M. Appel, J. A. S. Roberts, M. L. Helm, U. J. Kilgore, J. Y. Yang, D. L. DuBois and C. P. Kubiak, *J. Am. Chem. Soc.*, 2011, **133**, 12767-12779.
75. (a) S. Chen, R. Rousseau, S. Raugei, M. Dupuis, D. L. DuBois and R. M. Bullock, *Organometallics*, 2011, **30**, 6108-6118; (b) S. Chen, M.-H. Ho, R. M. Bullock, D. L. DuBois, M. Dupuis, R. Rousseau and S. Raugei, *ACS Catalysis*, 2013, accepted for publication.
76. (a) J. M. Savéant and E. Vianello, *Electrochim. Acta*, 1965, **10**, 905-920; (b) J. M. Savéant and E. Vianello, *Electrochim. Acta*, 1967, **12**, 629-646; (c) R. S. Nicholson and I. Shain, *Anal. Chem.*, 1964, **36**, 706-723; (d) A. J. Bard and L. R. Faulkner, *Electrochemical Methods: Fundamentals and Applications*, John Wiley & Sons, 2001.
77. J. A. S. Roberts and R. M. Bullock, *Inorg. Chem.*, 2013, **52**, 3823-3835.
78. A. M. Appel, D. H. Pool, M. O'Hagan, W. J. Shaw, J. Y. Yang, M. Rakowski DuBois, D. L. DuBois and R. M. Bullock, *ACS Catalysis*, 2011, **1**, 777-785.
79. (a) M. L. Helm, M. P. Stewart, R. M. Bullock, M. Rakowski DuBois and D. L. DuBois, *Science*, 2011, **333**, 863-866; (b) M. P. Stewart, M.-H. Ho, S. Wiese, M. L. Lindstrom, C. E. Thogerson, S. Raugei, R. M. Bullock and M. L. Helm, *J. Am. Chem. Soc.*, 2013, **135**, 6033-6046.
80. G. A. N. Felton, R. S. Glass, D. L. Lichtenberger and D. H. Evans, *Inorg. Chem.*, 2006, **45**, 9181-9184.
81. K. Haav, J. Saame, A. Kütt and I. Leito, *Eur. J. Org. Chem.*, 2012, 2167-2172.
82. T. Liu, D. L. DuBois and R. M. Bullock, *Nature Chemistry*, 2013, **5**, 228-233.
83. D. H. Pool, M. P. Stewart, M. J. O'Hagan, W. J. Shaw, J. A. S. Roberts, R. M. Bullock and D. L. DuBois, *Proc. Natl. Acad. Sci. U.S.A.*, 2012, **109**, 15634-15639.
84. V. Fourmond, P.-A. Jacques, M. Fontecave and V. Artero, *Inorg. Chem.*, 2010, **49**, 10338-10347.
85. A. M. Appel, S.-J. Lee, J. A. Franz, D. L. DuBois, M. Rakowski DuBois and B. Twamley, *Organometallics*, 2009, **28**, 749-754.
86. (a) T. Richardson, S. de Gala, R. H. Crabtree and P. E. M. Siegbahn, *J. Am. Chem. Soc.*, 1995, **117**, 12875-12876; (b) R. H. Crabtree, P. E. M. Siegbahn, O. Eisenstein, A. L. Rheingold and T. F. Koetzle, *Acc. Chem. Res.*, 1996, **29**, 348-354; (c) R. Custelcean and J. E. Jackson, *Chem. Rev.*, 2001, **101**, 1963-1980.
87. S. Horvath, L. E. Fernandez, A. M. Appel and S. Hammes-Schiffer, *Inorg. Chem.*, 2013, **52**, 3643-3652.
88. (a) F. A. Armstrong, N. A. Belsey, J. A. Cracknell, G. Goldet, A. Parkin, E. Reisner, K. A. Vincent and A. F. Wait, *Chem. Soc. Rev.*, 2009, **38**, 36-51; (b) C. L. McIntosh, F. Germer, R. Schulz, J. Appel and A. K. Jones, *J. Am. Chem. Soc.*, 2011, **133**, 11308-11319.
89. M. Frey, *ChemBioChem*, 2002, **3**, 153-160.
90. (a) M. H. V. Huynh and T. J. Meyer, *Chem. Rev.*, 2007, **107**, 5004-5064; (b) D. R. Weinberg, C. J. Gagliardi, J. F. Hull, C. F. Murphy, C. A. Kent, B. C. Westlake, A. Paul, D. H. Ess, D. G. McCafferty and T. J. Meyer, *Chem. Rev.*, 2012, **112**, 4016-4093; (c) S. Hammes-Schiffer, *Acc. Chem. Res.*, 2009, **42**, 1881-1889; (d) J. J. Warren, T. A. Tronic and J. M. Mayer, *Chem. Rev.*, 2010, **110**, 6961-7001; (e) J. M. Mayer, *Annu. Rev. Phys. Chem.*, 2004, **55**, 363-390; (f) C. J. Chang, M. C. Y. Chang, N. H. Damrauer and D. G. Nocera, *Biochem. Biophys. Acta*, 2004, **1655**, 13-28; (g) S. Hammes-Schiffer and N. Iordanova, *Biochim. Biophys. Acta*, 2004, **1655**, 29-36; (h) S. Hammes-Schiffer, *Acc. Chem. Res.*, 2001, **34**, 273-281.
91. S. Wiese, U. J. Kilgore, M.-H. Ho, S. Raugei, D. L. DuBois, R. M. Bullock and M. L. Helm, *ACS Catalysis*, 2013, 2527-2535.
92. W. A. Hoffert, J. A. S. Roberts, R. M. Bullock and M. L. Helm, *Chem. Commun.*, 2013, **49**, 7767-7769.
93. (a) G. M. Jacobsen, J. Y. Yang, B. Twamley, A. D. Wilson, R. M. Bullock, M. Rakowski DuBois and D. L. DuBois, *Energy Environ. Sci.*, 2008, **1**, 167-174; (b) E. S. Wiedner, J. Y. Yang, W. G. Dougherty, W. S. Kassel, R. M. Bullock, M. Rakowski DuBois and D. L. DuBois, *Organometallics*, 2010, **29**, 5390-5401; (c) E. S. Wiedner, J. A. S. Roberts, W. G. Dougherty, W. S. Kassel, D. L. DuBois and R. M. Bullock, *Inorg. Chem.*, 2013, **52**, 9975-9988.
94. T. Liu, S. Chen, M. J. O'Hagan, M. Rakowski DuBois, R. M. Bullock and D. L. DuBois, *J. Am. Chem. Soc.*, 2012, **134**, 6257-6272.
95. N. Wang, M. Wang, Y. Wang, D. Zheng, H. Han, M. S. G. Ahlquist and L. Sun, *J. Am. Chem. Soc.*, 2013, **135**, 13688-13691.
96. E. B. Hulley, K. D. Welch, A. M. Appel, D. L. DuBois and R. M. Bullock, *J. Am. Chem. Soc.*, 2013, **135**, 11736-11739.
97. C. T. Carver, B. D. Matson and J. M. Mayer, *J. Am. Chem. Soc.*, 2012, **134**, 5444-5447.
98. B. D. Matson, C. T. Carver, A. Von Ruden, J. Y. Yang, S. Raugei and J. M. Mayer, *Chem. Commun.*, 2012, **48**, 11100-11102.
99. (a) D. K. Dogutan, S. A. Stoian, R. McGuire, M. Schwalbe, T. S. Teets and D. G. Nocera, *J. Am. Chem. Soc.*, 2010, **133**, 131-140; (b) R. McGuire Jr, D. K. Dogutan, T. S. Teets, J. Suntivich, Y. Shao-Horn and D. G. Nocera, *Chemical Science*, 2010, **1**, 411-414.
100. (a) M. T. Mock, S. Chen, R. Rousseau, M. J. O'Hagan, W. G. Dougherty, W. S. Kassel, D. L. DuBois and R. M. Bullock, *Chem. Commun.*, 2011, **47**, 12212-12214; (b) C. J. Weiss, A. N. Groves, M. T. Mock, W. G. Dougherty, W. S. Kassel, M. L. Helm, D. L. DuBois and R. M. Bullock, *Dalton Transactions*, 2012, **41**, 4517-4529; (c) Z. M. Heiden, S. Chen, M. T. Mock, W. G. Dougherty, W. S. Kassel, R. Rousseau and R. M. Bullock, *Inorg. Chem.*, 2013, **52**, 4026-4039; (d) M. T. Mock, S. Chen, M. O'Hagan, R. Rousseau, W. G. Dougherty, W. S. Kassel and R. M. Bullock, *J. Am. Chem. Soc.*, 2013, **135**, 11493-11496.

Hydrogen Production

$$H^+ + H^- \longrightarrow H_2$$